NASA-TM-81354 19810009523

NASA Technical Memorandum 81354

DESCRIPTION OF THE HiMAT TAILORED COMPOSITE STRUCTURE AND LABORATORY MEASURED VEHICLE SHAPE UNDER LOAD

Richard C. Monaghan

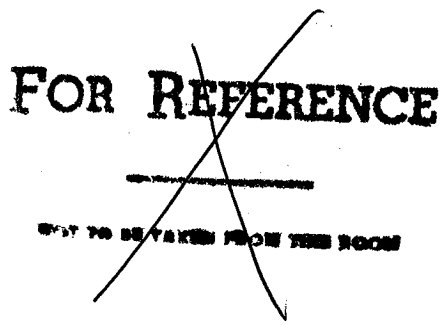

February 1981

NASA

NASA Technical Memorandum 81354

DESCRIPTION OF THE HiMAT TAILORED COMPOSITE STRUCTURE AND LABORATORY MEASURED VEHICLE SHAPE UNDER LOAD

Richard C. Monaghan

Dryden Flight Research Center
Edwards, California

National Aeronautics and
Space Administration

DESCRIPTION OF THE HiMAT TAILORED COMPOSITE STRUCTURE AND LABORATORY MEASURED VEHICLE SHAPE UNDER LOAD

Richard C. Monaghan
Dryden Flight Research Center

INTRODUCTION

The performance goals of modern aircraft require a wide variation in lifting surface aerodynamics for cruising, maneuvering, and take off and landing conditions. These variations are achieved primarily using leading and trailing edge flaps. An alternate method of achieving the required lifting surface aerodynamics is through an aeroelastically tailored structure. Such a structure would use the natural aerodynamic forces themselves to elastically reshape the geometry for obtaining the desired aerodynamics at a given flight condition.

Almost any structural material can be aeroelastically tailored to some degree. The laminated fibrous composites, however, are ideally suited to aeroelastic tailoring because the material properties of a laminate can be designed, through variations in the laminate layup, to meet a wide range of anisotropic requirements (ref. 1). Graphite-epoxy laminates, which generally produce lighter weight structures, have achieved widespread use as fiber dominated tailored structural laminates primarily for direct replacement of existing metallic structures. The HiMAT structurally tailored outer wing and canard use a matrix dominated structural laminate. Very little laboratory or flight data have been published related to these matrix dominated laminates. A description of the HiMAT structural design methodology along with ground test data is included in reference 2.

This report is intended to provide a detailed documentation of the aeroelastically tailored outer wing and canard structure of the HiMAT vehicle as well as a general description of the overall aircraft structure. Laboratory measured outer wing and canard twist under a simulated flight load is compared with design predictions.

AIRCRAFT GENERAL DESCRIPTION

Two HiMAT research vehicles (fig. 1) have been designed and fabricated and are presently in flight test. These vehicles are 0.44-scale remotely piloted powered models of a 7700 kilogram (17,000 pound) fighter type vehicle. They have a wing span of 4.74 meters (15.56 feet) a length of 6.06 meters (19.88 feet) and a mass of 1385 kilograms (94.9 slugs). They were designed to be air launched from a B-52 airplane. The primary objectives of the vehicles were to achieve a sustained turn capability of 8g at 0.9 Mach number and 25,000 feet, and a 3 minute sustained flight at 1.4 Mach number. The vehicles have 10 control surfaces (5 on each side) including canard flaps, ailerons, elevons, elevators, and twin all-flying vertical tails. Each surface is capable of being actuated independently or in any combination through an onboard computer which receives its commands via telemetry from a ground-based cockpit. The HiMAT vehicles are powered by single J85-21 afterburning turbojet engines.

MATERIAL PROPERTIES

Composites comprise a large percentage of the HiMAT structure. For the tailored composites used on HiMAT there are no published or widely accepted material properties. The laminate properties for the final structural design were analytically generated by the contractor using the lamina properties listed in table 1. The analytical method used is basically that outlined in reference 1.

STRUCTURE

General

An exploded view of the aircraft structure is shown in figure 2. The fuselage and inboard wing consist of an aluminum frame structure with mechanically fastened graphite-epoxy honeycomb covers. Two major titanium frames carry the wing loads through the fuselage; the rear frame of the two provides the structure for the main engine mounts. The engine exhaust fairing is constructed from titanium frames and skins. Fuel is carried integrally in the fuselage and inboard wing structure from the aft bulkhead of the avionics bay to the aft wing carry-through frame.

The tail booms and the main landing gear are tied into a box formed by two substantial titanium wing ribs. The outer most of these ribs also form the attachment for the outboard wing.

The control surfaces are full depth honeycomb with graphite-epoxy covers. The surfaces located on the outboard wing and canard will be described in more detail in the following sections.

The wing tip fin is an aluminum cast frame with graphite-epoxy honeycomb bonded into the cutout sections. The tip fin is mechanically fastened to the wing tip. Large radius fiber glass fairings are used top and bottom to blend the two parts together.

Outer Wing

The major effort to aeroelastically tailor the vehicle was done on the outer wing structure. The structural layout, as shown in figure 3, consists of a central structural box, a fixed leading edge flap, and trailing edge control surfaces. The structural box is constructed of tailored covers of AS/3501-5 graphite-epoxy layed up with generally 40% at 50^{o}, and 20% at 35^{o} with respect to the laminate reference axis. Table 2 lists the exact ply layup. The number in the column labeled "Ply number" indicates the sequence of the layup starting from the outer surface. The second number is either a 1 or a 2. A 1 indicates a ply that starts inboard and a 2 indicate a ply that occupies the same layer but starts outboard of the termination of the inboard ply. A number of plys of boron epoxy are interlayed locally to reinforce the root attachment, and a number of plys of fiber glass-epoxy are interlayed locally at the tip to reinforce the attachment to the tip fin. The box structure is closed out by leading and trailing edge spars constructed of T300/934 graphite-epoxy. All plys are layed at 45^{o} to the centerline of the spar except for one cap and web ply on the leading edge between the root and X_F = 166.8 cm (46.0 in.) which is at 90^{o} (F refers to the fuselage-wing Cartesian coordinate reference system). The number of cap (c) plys and web (w) plys along the spars is indicated in figure 3(b). The root rib is also T300/934 graphite-epoxy three plys thick. The tip reduces to a thin cross section locally for the tip fin connection with a solid fiber glass filler inserted between the skins at the bolt lines. The core of the structural box is full depth aluminum honeycomb. The wing box is a 100% bonded structure.

The leading edge of the outboard wing (fig. 3(c)) is constructed of fiber glass-epoxy. The layup is constant spanwise and varies chordwise (table 3). It is attached to the wing box by a full length piano hinge at both the top and bottom surfaces. To increase the effective sing twist, the leading edge is cut into three segments with single pin connections near the nose, and the attachment hinges are cut into approximately 10 cm (4 in.) segments.

The elevon and aileron structures are similar having T300/934 graphite-epoxy skins, and a channel of the same material for the leading edge close out. The surfaces are mounted to the wing box on self-aligning ball hinges. The elevon is mounted at only two hinge points so that it does not contribute to the strength or stiffness of the outboard wing. The aileron is, however, mounted at three points and must be accounted for. The aileron skin thickness is shown in figure 3(c). One full length ply is layed out at 0^{o} to the hinge line and the rest at $\pm 45^{o}$. The leading edge closeout channel is broken into segments between aluminum hinge fittings and is five plys thick with one ply at 0^{o} and the rest at $\pm 45^{o}$.

Canard

The canard (fig. 4) is also an aeroelastically tailored surface with structural layout similar to the wing. All the coordinates in figure 4 are referenced to the plane of the canard, which is installed at a 20° dihedral to the wing-fuselage reference plane. The equations relating the canard reference system to the fuselage reference system are:

$$X_C = X_F / \cos 20^{\circ} - 27.03 \text{ cm } (10.64 \text{ in.})$$

$$Y_C = Y_F - 116.8 \text{ cm } (46.0 \text{ in.})$$

The canard structural box consists of AS/3501-5 graphite-epoxy for covers layed up primarily at $\pm 45^{\circ}$ and 15° with respect to the laminate reference axis. These covers extend to the trailing edge outboard of the canard flap. The upper skin includes a cutout at the outer end of the canard flap requiring significant local reinforcement. The skin layups and reinforcement layups are listed in table 4a and 4b, respectively. A number of layers of boron epoxy are interlayed locally in the area where the structural box covers are mechanically fastened to the titanium main fitting. The box is closed out by T300/934 graphite-epoxy leading and trailing edge spars. The spar ply layup is consistent along the entire span (fig. 4(b)) with all plys at $\pm 45^{\circ}$ with reference to the centerline of the spars. The leading edge spar cap from the root to X_C = 41 cm (16 in.) tapers slightly. Elsewhere, the leading and trailing edge spar caps are of constant width. The root is closed out with an aluminum rib between the main fitting and the leading edge fitting. The tip is closed out with a solid aluminum rib, which was originally designed to support a tip mass. The canard box, like the wing, is a 100% bonded structure.

The leading edge of the canard is constructed of T300/934 graphite-epoxy. It is attached to the canard box by closely spaced screws both top and bottom. The leading edge is cut into four segments. One ply layup is used on the inboard two segments, and another ply layup is used on the outboard two segments (table 5).

The canard flap is constructed with a stainless steel front half and a T300/934 graphite-epoxy honeycomb rear half. The flap is hinged at only two points so that it contributes no stiffness or strength to the canard structure.

DESIGN VERIFICATION TEST

General

A primary goal in the structural design of the outer wing and the canard was to achieve an aerodynamically favorable spanwise twist distribution for maneuvering flight conditions.

Final structural design analysis was accomplished using the NASTRAN finite element computer code. A general view of the NASTRAN structural model of the HiMAT vehicle is shown in figure 5. Details of the outer wing and canard structural models are shown in figure 6(a) and (b), respectively. Coordinates for the outer wing and canard grid points are listed in tables 6a and b. The NASTRAN program was used to compute structural deflections at each model grid point. Verification of these deflections was accomplished by performing a loads test prior to delivery of the vehicle to NASA.

TEST CONDITIONS

The verification loads test consisted of an 8g distributed load on the outer wing and canard along with point loads on the wing tip fin and rudder, which represented the resultant 8g forces on each of these surfaces. All loads were applied simultaneously in increments up to 100% load. A second test was made which increased the same load distribution to 110% of the 8g load. The 8g loads applied are included in table 7 and in figure 7. The outer wing and canard loads are applied in tension through a series of whiffletrees and hydraulic jacks using vacuum and glue on loading pads. The point loads on the wing tip fin and rudder were applied by an individual hydraulic jack at each load point.

For the verification test, the HiMAT structure was fully assembled with the maneuver leading edges installed. The engine was removed and the control system was connected to an external fluid pressure source. The vehicle was supported in an upright position by an overhead structure through its launch hooks. A reaction opposite to the test load was provided by a beam which attached to the engine mounts and extended out through the tailcone where a hydraulic actuator produced the desired restraining action about a fulcrum. The vehicle was also restrained from rolling through this beam as well as through the nose landing gear fitting.

Prior to gathering data, a zero load condition was established by hydraulically biasing the load system for the outer wing and canard to support the weight of the whiffletree and local vehicle structure.

DISCUSSION OF RESULTS

Deflection measurements were made at 31 locations on the left-hand outer wing and 24 locations on the left-hand canard. These were distributed along the leading and trailing edges and the forward and aft spars. Measurements were also taken along the centerline of the fuselage and at selected points on the right-hand side of the vehicle. The location of each measurement along with the vertical displacement measured at the 8g load condition are listed in table 8. Hysteresis in the structure and the test setup was minimized by using the 110% load test and averaging the data recorded as the load increased through the 8g test condition with the data recorded as the load decreased back through the 8g test condition. The loads applied to the vehicle for the verification test load were substituted into the NASTRAN computer model. The

deflections predicted by NASTRAN are listed in table 9 and correspond to the locations identified by the computer model coordinates listed in table 6. Using predicted and measured deflections, spanwise twist distributions were plotted for the outer wing and canard (fig. 8). The accuracy of the measured points in the figures is estimated to be within ±0.1° based on the linearity and accuracy of the instrumentation and the vehicle dimensions. Repeatability of the data from the 100% load test and the 110% load test also fell within this same accuracy band. The pitch rotation of the vehicle on its support structure was within 0.02° of the NASTRAN prediction.

Measurements between the forward and aft spars on both the outer wing and canard (fig. 8) indicate the actual (measured) twist to be less than the predicted (NASTRAN) twist. The percentage of error between these spanwise twist distribution is similar for both the wing and canard.

Figure 9 presents canard and wing chordwise vertical deflections at several span stations for the averaged 100% load condition.[1] The deflections measured at the wing and canard tips were made on structure which is reasonably rigidly attached to the respective main box structures, and correlates well with the twist measurements made between the spars. Twist comparisons also appear to be valid for the canard outboard of the canard flap, however nonstructural movement included in the measurements on the control surfaces make similar comparison invalid elsewhere.

An assessment of the relative angle of the wing leading edge to the plane of the wing structural box (fig. 9(a)) indicates the fiber glass-epoxy leading edge to be more flexible than predicted. Similar measurements on the canard (fig. 9(b), which incorporates a graphite-epoxy leading edge and a different attachment method, indicates good agreement between measured and predicted data.

The limited data available for the right wing are shown by the solid symbols in figures 8 and 9. These data indicate that the vehicle may have rolled slightly to the left under load. However, small differences observed in deflections and twist are within the stated accuracy of the data.

Data contained in reference 1 suggest that differences between predicted and measured parameters on the outer wing and canard may be due to discrepancies in material properties input to the NASTRAN program and/or the nonlinear nature of the stress strain relationship of the HiMAT composite layup.

[1]The chordwise deflections at span station 86.4 cm (34.0 in.) are actually on the inboard wing, and are presented here as a reference to assess the stiffness of the inboard wing as compared with the outboard wing. Additional inboard wing deflection data can be found in table 8.

CONCLUDING REMARKS

One of the major design features of the HiMAT vehicle is an aeroelastically tailored outer wing and canard. A detailed description of these structures along with a general description of the overall structure of the vehicle is provided. Test data in the form of laboratory measured twist under load and predicted twist from the HiMAT NASTRAN structural design program are compared. The results of this comparison indicate that the measured twist is generally less than the NASTRAN predicted twist. These discrepancies in twist predictions are attributed, at least in part, to the inability of current analytical composite materials programs to provide sufficiently accurate properties of matrix dominated laminates for input into structural programs such as NASTRAN.

Discrepancies in wing twist are expected to have only a minor effect on the attainment of the performance goal for the HiMAT program (approximately a 1% increase in drag at the maneuver design point). However, the technology being demonstrated will have significant inpact on more critical aerodynamic-aeroelastic interactive designs such as the current efforts on the forward-swept wing. Improvement in composite material analytical design tools and further laboratory component testing are essential if aeroelastically tailored composites are to be fully utilized in future designs.

REFERENCES

1. Advanced Composites Design Guide. Vols. I to V. Third ed. U.S. Air Force Materials Lab., Wright-Patterson Air Force Base, Jan. 1973.

2. Price, M. A.: HiMAT Structural Development Design Methodology. NASA CR-144886, 1979.

TABLE 1. MATERIAL PROPERTIES OF COMPOSITES AT ROOM TEMPERATURE

Property	Fiber ref.	AS/3501-5 Graphite-epoxy unidirectional tape	T300/934 Graphite-epoxy fabric	7781 Fiber glass-epoxy fabric
Ultimate tensile strength, MN/m^2 (ksi)	0°	1455 (211)	421 (61)	345 (50)
	90°	53 (7.7)	421 (61)	276 (40)
Ultimate compressive strength, MN/m^2 (ksi)	0°	1455 (211)	379 (55)	476 (69)
	90°	221 (32.1)	379 (55)	393 (57)
Ultimate shear strength, MN/m^2 (ksi)		71 (10.3)	41 (5.1)	86 (12.5)
Modulous of elasticity, MN/m^2 (ksi)	0°	138,000 (20,000)	72,000 (10,450)	26,500 (3,850)
	90°	10,300 (1,490)	72,000 (10,450)	26,500 (3,850)
Shear modulous, MN/m^2 (ksi)		2,400 (350)	4,500 (660)	11,200 (1,620)
Poisson's ratio		0.30	0.51	0.14
Lamina thickness, cm (in.)		0.013 (0.0052)	0.033 (0.013)	0.023 (0.009)

TABLE 2a. COMPOSITE SKIN LAYUP FOR OUTBOARD WING STRUCTURAL BOX, PLYS ORIGINATING FROM X_F = 102.4 cm (40.3 in)

Ply number	Material (1)	Fiber orientation, deg (2)	Length of ply, cm (in) (2)	Angle of termination of ply, deg (2)
1-1	Gr	50	153.7 (60.5)	cont
2-1	Gr	-50	153.7 (60.5)	cont
3-1	Gr	35	153.7 (60.5)	cont
4-1	B	0	18.0 (7.1)	129.3
5-1	B	0	17.2 (6.8)	129.3
6-1	Gr	-50	153.7 (60.5)	cont
7-1	Gr	50	153.7 (60.5)	cont
8-1	B	90	16.1 (6.4)	129.3
9-1	Gr	50	153.7 (60.5)	cont
10-1	Gr	-50	153.7 (60.5)	cont
11-1	Gr	35	153.7 (60.5)	cont
12-1	B	0	15.1 (6.0)	129.3
13-1	B	0	14.2 (5.6)	129.3

[1] Gr-graphite-epoxy, B-boron epoxy, Gl-glass-epoxy

[2] Measured with respect to wing laminate referance axis

TABLE 2a. CONTINUED

Ply Number	Material (1)	Fiber Orientation, deg (2)	Length of Ply, cm (in) (2)	Angle of termination of ply, deg (2)
14-1	Gr	-50	130.6 (51.4)	90
15-1	Gr	50	129.8 (51.1)	90
16-1	B	90	13.2 (5.2)	129.3
17-1	Gr	50	97.7 (38.45)	90
18-1	Gr	-50	96.9 (38.15)	90
19-1	Gr	35	89.5 (35.25)	90
20-1	Gr	50	12.2 (4.8)	129.3
21-1	B	0	11.2 (4.4)	129.3
22-1	Gr	50	73.2 (28.8)	90
23-1	Gr	-50	72.1 (28.4)	90
24-1	B	0	10.2 (4.0)	129.3
25-1	B	0	9.1 (3.6)	129.3
26-1	Gr	50	40.6 (16.0)	90
27-1	Gr	-50	39.6 (15.6)	90
28-1	Gr	-50	64.8 (25.5)	90

TABLE 2a. CONTINUED

Ply Number	Material (1)	Fiber Orientation, deg (2)	Length of Ply, cm (in) (2)	Angle of termination of Ply, deg (2)
29-1	Gr	50	64.0 (25.2)	90
30-1	B	0	9.1 (3.6)	129.3
31-1	B	0	10.2 (4.0)	129.3
32-1	Gr	-50	81.3 (32.0)	90
33-1	Gr	50	80.5 (31.7)	90
34-1	B	0	11.2 (4.4)	129.3
35-1	Gr	50	12.2 (4.8)	129.3
36-1	Gr	35	88.6 (34.9)	90
37-1	Gr	-50	105.9 (41.7)	90
38-1	Gr	50	105.2 (41.4)	90
39-1	B	90	13.2 (5.2)	129.3
40-1	Gr	50	114.3 (45.0)	90
41-1	Gr	-50	113.3 (44.6)	90
42-1	B	0	14.2 (5.6)	129.3
43-1	B	0	15.2 (6.0)	129.3

TABLE 2a. CONCLUDED

Ply Number	Material (1)	Fiber Orientation, deg (2)	Length of Ply, cm (in) (2)	Angle of termination of Ply, deg (2)
44-1	Gr	35	153.7 (60.5)	cont.
45-1	Gr	-50	153.7 (60.5)	cont.
46-1	Gr	50	153.6 (60.5)	cont.
47-1	B	90	16.3 (6.4)	129.3
48-1	Gr	50	153.7 (60.5)	cont.
49-1	Gr	-50	153.7 (60.5)	cont.
50-1	B	0	153.7 (60.5)	129.3
51-1	B	0	18.0 (7.1)	129.3
52-1	Gr	35	153.7 (60.5)	cont.
53-1	Gr	-50	153.7 (60.5)	cont.
54-1	Gr	50	153.7 (60.5)	cont.

TABLE 2b. COMPOSITE SKIN LAYUP FOR OUTBOARD WING STRUCTURAL BOX, PLYS ORIGINATING FROM X_F = 221.2 cm (87.1 in)

Ply Number	Material (1)	Fiber Orientation, deg (2)	Length of Ply, cm (in) (2)	Angle of termination of Ply, deg (2)
4-2	Gl	0	15.2 (6.0)	129.3
8-2	Gl	0	14.2 (5.6)	129.3
12-2	Gl	0	13.2 (5.2)	129.3
14-2	Gl	-50	11.9 (4.7)	129.3
15-2	Gl	50	10.7 (4.2)	129.3
16-2	Gl	-50	9.6 (3.8)	129.3
17-2	Gl	0	8.6 (3.4)	129.3
38-2	Gl	0	8.6 (3.4)	129.3
39-2	Gl	-50	9.6 (3.8)	129.3
40-2	Gl	50	10.7 (4.2)	129.3
41-2	Gl	-50	11.9 (4.7)	129.3
43-2	Gl	0	13.2 (5.2)	129.3
47-2	Gl	0	14.2 (5.6)	129.3
51-2	Gl	0	15.2 (6.0)	129.3

TABLE 3. WING LEADING EDGE COMPOSITE LAYUP

Ply Number (1)	Ply Orientation, deg (2)	Ply Termination, cm (in) (3)
1	45	continuous
2	-45	continuous
3	0	continuous
4	90	11.94 (4.70)
5	-45	8.26 (3.25)
6	45	7.87 (3.10)
7	0	7.49 (2.95)
8	90	7.11 (2.80)
9	0	6.73 (2.65)
10	90	6.35 (2.50)
11	0	5.97 (2.35)
12	90	5.59 (2.20)
13	90	5.21 (2.05)
14	90	4.83 (1.90)
15	0	4.45 (1.75)
16	90	4.06 (1.60)
17	0	3.68 (1.45)
18	45	3.30 (1.30)
19	-45	2.92 (1.15)
20	90	2.54 (1.00)
21	0	continuous
22	-45	continuous
23	45	continuous

[1] Number sequence from outer ply to inner ply

[2] Measured with respect to the leading edge spar

[3] Measured from and perpendicular to the web of the leading edge spar

TABLE 4a. COMPOSITE SKIN LAYUP FOR CANARD STRUCTURAL BOX, EXCLUDING UPPER SKIN REINFORCEMENT AROUND CUTOUT

Ply number	Material [1]	Fiber orientation, deg [2]	Start of ply [2]		End of ply [2]	
			$X_{CL'}$ cm (in)	Angle, deg	$X_{CL'}$ cm (in)	Angle, deg
1-1	Gr	45	9.4 (3.7)	143	152.9 (60.2)	137
2-1	Gr	-45	9.4 (3.7)	143	152.9 (60.2)	137
3-1	Gr	15	9.4 (3.7)	143	152.9 (60.2)	137
4-1	Gr	-45	9.4 (3.7)	143	55.4 (21.8)	90
5-1	Gr	45	9.4 (3.7)	143	69.6 (27.4)	90
6-1	B	0	17.5 (6.9)	60	45.7 (18.0)	90
7-1	B	0	23.4 (9.2)	90 [3]	45.2 (17.8)	90
8-1	B	0	18.3 (7.2)	60	44.7 (17.6)	90
9-1	Gr	45	9.4 (3.7)	143	56.9 (22.4)	90
10-1	Gr	15	9.4 (3.7)	143	152.9 (60.2)	137
11-1	Gr	45	33.5 (13.2)	90	65.5 (25.8)	90
12-1	B	90	19.3 (7.6)	60	44.2 (17.4)	90
13-1	Gr	45	9.4 (3.7)	143	54.9 (21.6)	90

[1] Gr-graphite, B-boron

[2] Measured with respect to the canard laminate reference axis

$$X_{CL} = (X_C/\cos 47^\circ)(Y_C - X_C \tan 47^\circ) \sin 47^\circ$$

$$Y_{CL} = (Y_C - X_C \tan 47^\circ) \cos 47^\circ$$

[3] Start of ply is trimmed at corner to match 60° angle of adjacent ply intersection

TABLE 4a. CONTINUED

Ply number	Material (1)	Fiber orientation, deg (2)	Start of ply (2)		End of ply (2)	
			$X_{CL'}$ cm (in)	Angle, deg	$X_{CL'}$ cm (in)	Angle, deg
14-1	Gr	45	9.4 (3.7)	143	61.5 (24.2)	90
14-1	Gr	45	101.6 (40.0)	90	152.9 (60.2)	137
15-1	Gr	45	21.3 (8.4)	137	52.3 (20.6)	90
15-2	B	90	9.4 (3.7)	143	21.3 (8.4)	137
16-1	B	0	20.1 (7.9)	60 (3)	43.7 (17.2)	90
17-1	B	0	25.4 (10.0)	90	43.2 (17.0)	90
18-1	B	0	20.8 (8.2)	60	42.7 (16.8)	90
19-1	B	0	21.8 (8.6)	60	42.2 (16.6)	90
20-1	Gr	45	37.6 (14.8)	90	49.5 (19.5)	90
21-1	Gr	-45	9.4 (3.7)	143	48.8 (19.2)	90
22-1	Gr	45	40.4 (15.9)	90	47.2 (18.6)	90
22-2	B	90	9.4 (3.7)	143	40.4 (15.9)	90
23-1	Gr	-45	12.2 (4.8)	60	65.5 (25.8)	90
24-1	Gr	45	13.0 (5.1)	60	45.0 (17.7)	90
25-1	Gr	15	14.0 (5.5)	60	152.9 (60.2)	137
26-1	Gr	45	14.7 (5.8)	60	42.9 (16.9)	90

TABLE 4a. CONTINUED

Ply number	Material (1)	Fiber orientation, deg (2)	Start of Ply (2)		End of Ply (2)	
			$X_{CL'}$ cm (in)	Angle, deg	$X_{CL'}$ cm (in)	Angle, deg
27-1	Gr	45	15.7 (6.2)	60	57.7 (22.7)	90
28-1	Gr	15	16.5 (6.5)	60	52.8 (20.8)	90
28-1	Gr	15	97.0 (38.2)	90 (3)	120.9 (47.6)	90
29-1	Gr	45	31.5 (12.4)	90	152.9 (60.2)	137
30-1	Gr	15	16.5 (6.5)	60	57.7 (22.7)	90
30-1	Gr	15	97.0 (38.2)	90	120.9 (47.6)	90
31-1	Gr	45	15.7 (6.2)	60	61.5 (24.2)	90
32-1	Gr	45	14.7 (5.8)	60	41.9 (16.5)	90
33-1	Gr	15	14.0 (5.5)	60	152.9 (60.2)	137
34-1	Gr	45	13.0 (5.1)	60	43.9 (17.3)	90
35-1	Gr	15	12.2 (4.8)	60	47.2 (18.6)	90
36-1	Gr	45	40.4 (15.9)	90	46.0 (18.1)	90
36-2	B	90	9.4 (3.7)	143	40.4 (15.9)	90
37-1	Gr	-45	9.4 (3.7)	143	45.5 (17.9)	90
38-1	Gr	45	35.6 (14.0)	90	48.3 (19.0)	90

TABLE 4a. CONTINUED

Ply number	Material (1)	Fiber orientation, deg (2)	Start of Ply (2)		End of Ply (2)	
			$X_{CL'}$ cm (in)	Angle, deg	$X_{CL'}$ cm (in)	Angle, deg
39-1	B	0	21.8 (8.6)	60	42.2 (16.6)	90
40-1	B	0	20.8 (8.2)	60	42.7 (16.8)	90
41-1	B	0	27.4 (10.8)	90 (3)	43.2 (17.0)	90
42-1	B	0	20.1 (7.9)	60	43.7 (17.2)	90
43-1	Gr	45	21.3 (8.4)	137	50.8 (20.0)	90
43-2	B	90	9.4 (3.7)	143	21.3 (8.4)	137
44-1	Gr	-45	9.4 (3.7)	143	42.4 (16.7)	90
44-1	Gr	-45	101.6 (40.0)	90	152.9 (60.2)	137
45-1	Gr	45	9.4 (3.70)	143	54.1 (21.3)	90
46-1	B	90	19.3 (7.6)	60	44.2 (17.4)	90
47-1	Gr	45	39.6 (15.6)	90	65.5 (25.8)	90
48-1	Gr	15	9.4 (3.7)	143	152.9 (60.2)	137
49-1	Gr	45	9.4 (3.7)	143	56.4 (22.2)	90
50-1	B	0	18.3 (7.2)	60	44.7 (17.6)	90
51-1	B	0	29.5 (11.6)	90 [3]	45.2 (17.8)	90

TABLE 4a. CONCLUDED

Ply number	Material (1)	Fiber orientation, (2) deg	Start of Ply (2)		End of Ply (2)	
			$X_{CL'}$ cm (in)	Angle, deg	$X_{CL'}$ cm (in)	Angle, deg
52-1	B	0	17.5 (6.9)	60	45.7 (18.0)	90
53-1	Gr	45	9.4 (3.7)	143	69.6 (27.4)	90
54-1	Gr	-45	9.4 (3.7)	143	51.3 (20.2)	90
55-1	Gr	15	9.4 (3.7)	143	152.9 (60.2)	137
56-1	Gr	-45	9.4 (3.2)	143	152.9 (60.2)	137
57-1	Gr	45	9.4 (3.7)	143	152.9 (60.2)	137

TABLE 4b. COMPOSITE SKIN LAYUP FOR CANARD STRUCTURAL BOX, UPPER SKIN REINFORCEMENT AROUND CUTOUT

Ply number	Material ①	Fiber orientation ②, deg	Start of ply ②		End of ply ②	
			$X_{CL'}$ cm (in)	$Y_{CL'}$ cm (in)	$X_{CL'}$ cm (in)	$Y_{CL'}$ cm (in)
15-1	Gr	45	99.6 (39.2)	1.3 (0.5)	123.4 (48.6)	20.3 (8.0)
21-1	Gr	-45	100.1 (39.4)	1.8 (0.7)	122.9 (48.4)	19.8 (7.8)
26-1	Gr	45	100.6 (39.6)	3.3 (0.9)	122.4 (48.2)	19.3 (7.6)
32-1	Gr	45	101.1 (39.8)	2.8 (1.1)	121.9 (48.0)	18.8 (7.4)
37-1	Gr	-45	101.6 (40.0)	3.3 (1.3)	121.4 (47.8)	18.3 (7.2)
43-1	Gr	45	103.1 (40.2)	3.8 (1.5)	120.9 (47.6)	17.8 (7.0)

TABLE 5. CANARD LEADING EDGE COMPOSITE LAYUP

Inboard Segments

Ply [1] Number	Ply [2] Orientation, deg	Ply [3] Termination, cm (in)
1	0	continuous
2	45	continuous
3	135	5.08 (2.0)
4	90	4.57 (1.8)
5	45	4.06 (1.6)
6	135	3.56 (1.4)
7	90	3.05 (1.2)
8	135	2.54 (1.0)
9	45	2.03 (0.8)
10	0	continuous

Outboard Segments

Ply [1] Number	Ply [2] Orientation, deg	Ply [3] Termination, cm (in)
1	0	continuous
2	45	continuous
3	135	3.56 (1.4)
4	90	3.05 (1.2)
5	45	2.54 (1.0)
6	135	2.03 (0.8)
7	0	continuous

[1]Number sequence from outer ply to inner ply

[2]Measured with respect to the 25% chord

[3]Measured from and perpendicular to the 25% chord

TABLE 6a. WING GRID POINTS USED IN NASTRAN MODEL (COORDINATES IN INCHES)

GRID NUMBER	X_F	Y_F	Z_F
25	89.659	188.06	97.745
26	89.659	191.51	98.347
27	89.659	195.044	98.825
28	89.659	197.41	99.085
29	89.659	199.76	99.325
30	89.659	202.91	99.625
31	89.659	206.221	99.875
32	89.659	210.995	100.07
33	89.659	216.001	99.725
47	86.0	184.4	97.685
48	86.0	187.918	98.905
49	86.0	187.918	97.755
50	86.0	208.423	100.57
51	86.0	208.423	99.785
52	86.0	213.475	99.825
53	86.0	184.4	97.685
54	86.0	187.918	98.905
55	86.0	187.918	97.755
56	86.0	191.668	99.525
57	86.0	191.668	98.135
58	86.0	194.214	99.865
59	86.0	194.214	98.415
60	86.0	196.775	100.02
61	86.0	196.775	98.685
62	86.0	200.129	100.39
63	86.0	200.129	99.055
64	86.0	203.596	100.56
65	86.0	203.596	99.375
66	86.0	205.2	100.07
67	86.0	209.37	99.949

GRID NUMBER	X_F	Y_F	Z_F
68	86.0	213.475	99.825
69	83.7	203.549	100.10
70	81.791	206.420	99.987
71	79.90	209.264	99.872
72	84.504	198.992	100.42
73	84.504	198.992	99.072
74	82.9	201.372	100.66
75	82.9	201.372	99.313
79	82.562	193.972	100.12
80	82.562	193.972	98.713
81	84.977	186.914	98.901
82	84.977	186.914	97.741
83	84.988	193.331	99.876
84	84.988	193.331	98.413
85	83.924	195.082	100.08
86	83.924	195.082	98.698
87	82.481	197.455	100.47
88	82.481	197.455	99.096
89	80.95	199.973	100.72
90	80.95	199.973	99.274
91	80.279	200.895	100.14
92	78.127	203.853	100.02
93	76.10	206.641	99.902
94	83.85	189.684	99.544
95	83.85	189.684	98.131
96	82.644	191.283	99.904
97	82.644	191.283	98.409
98	81.359	192.990	100.16
99	81.359	192.990	98.725
100	79.628	195.287	100.54

TABLE 6a. CONTINUED

GRID NUMBER	X_F	Y_F	Z_F
101	79.628	195.287	99.129
102	77.80	197.713	100.71
103	77.80	197.713	99.395
104	76.70	198.528	100.18
105	74.681	201.438	100.05
106	72.70	204.295	99.928
109	84.509	182.909	97.676
110	82.824	184.801	98.894
111	82.824	184.801	97.712
112	80.9	186.926	99.567
113	80.9	186.926	98.095
114	79.659	188.673	99.941
115	79.659	188.673	98.404
116	78.319	190.511	100.25
117	78.319	190.511	98.735
118	76.548	192.946	100.63
119	76.548	192.946	99.166
120	74.7	195.489	100.66
121	74.7	195.489	99.576
122	74.051	196.375	100.22
123	71.817	199.431	100.08
124	69.75	202.258	99.951
140	81.109	179.509	97.615
141	79.385	181.425	98.883
142	79.385	181.425	97.665
143	77.35	183.687	99.585
144	77.35	183.687	98.074
145	76.028	185.504	100.00
146	76.028	185.504	98.397
147	74.595	187.473	100.33

GRID NUMBER	X_F	Y_F	Z_F
148	74.595	187.473	98.754
149	72.726	190.042	100.69
150	72.726	190.042	99.189
151	70.8	192.691	100.85
152	70.8	192.691	99.591
153	69.8	193.577	100.27
154	67.873	196.667	100.12
155	66.0	199.670	99.980
165	77.559	175.959	97.560
166	75.819	177.925	98.876
167	75.819	177.925	97.608
168	73.7	180.319	99.597
169	73.7	180.319	98.041
170	72.345	182.288	100.04
171	72.345	182.288	98.368
172	70.872	184.436	100.38
173	70.872	184.436	98.746
174	68.978	187.193	100.74
175	68.978	187.193	99.205
176	67.05	190.000	100.96
177	67.05	190.000	99.655
178	66.454	190.779	100.32
179	64.019	193.966	100.16
180	61.85	196.805	100.01
186	73.379	171.779	97.486
187	71.661	173.844	98.821
188	71.661	173.844	97.514
189	73.379	171.779	97.486
190	71.661	173.844	98.821
191	71.661	173.844	97.514

TABLE 6a. CONTINUED

GRID NUMBER	X_F	Y_F	Z_F
192	69.50	176.444	99.607
193	69.50	176.444	97.97
194	67.971	178.468	100.05
195	67.971	178.468	98.344
196	66.288	180.697	100.45
197	66.288	180.697	98.730
198	64.152	183.526	100.78
199	64.152	183.526	99.183
200	62.0	186.378	100.97
201	62.0	186.378	99.622
202	60.0	186.547	100.39
203	60.0	191.15	100.20
204	60.0	195.529	100.02
209	69.099	167.499	97.391
210	67.318	169.581	98.788
211	67.318	169.581	97.429
212	65.0	172.292	99.615
213	65.0	172.292	97.905
214	63.400	174.475	100.08
215	63.400	174.475	98.268
216	61.626	176.895	100.49
217	61.626	176.895	98.643
218	59.408	179.921	100.83
219	59.408	179.921	99.123
220	57.2	182.934	101.04
221	57.2	182.934	99.577
222	56.18	184.565	100.44
223	60.0	186.65	100.48
224	60.0	191.0	100.26
225	58.25	190.200	100.26

GRID NUMBER	X_F	Y_F	Z_F
226	54.45	188.464	100.27
227	60.0	195.35	100.05
228	56.6	194.107	100.09
229	52.60	192.645	100.14
239	64.8	163.203	97.364
240	62.925	165.268	98.779
241	62.925	165.268	97.281
242	60.4	168.048	99.665
243	60.4	168.048	97.762
244	58.699	170.370	100.20
245	58.699	170.370	98.166
246	56.802	172.960	100.67
247	56.802	172.960	98.632
248	54.458	176.159	101.02
249	54.458	176.159	99.144
250	52.15	179.311	101.16
251	52.15	179.311	99.525
252	50.55	181.493	100.39
253	48.68	185.828	100.28
254	46.60	190.452	100.22
255	60.3	158.784	97.116
256	58.396	160.823	98.816
257	58.396	160.823	97.092
259	60.3	158.784	97.116
260	58.396	160.823	98.816
261	58.396	160.823	97.092
262	55.7	163.712	99.953
263	55.7	163.712	97.767
264	53.889	166.169	100.52
265	53.889	166.169	98.111

TABLE 6a. CONTINUED

GRID NUMBER	X_F	Y_F	Z_F
266	51.857	168.927	100.95
267	51.857	168.927	98.637
268	49.375	172.296	101.23
269	49.375	172.296	99.087
270	46.95	175.580	101.29
271	46.95	175.580	99.457
272	45.15	178.546	100.34
273	42.90	183.187	100.29
274	40.30	188.15	100.30
275	45.80	169.579	101.39
276	45.80	169.579	99.003
277	45.80	174.755	101.33
278	45.80	174.755	99.411
279	54.4	152.955	96.990
280	52.534	155.068	99.022
281	52.534	155.068	96.935
282	49.75	158.222	100.40
283	49.75	158.222	97.652
284	47.786	160.838	101.00
285	47.786	160.838	98.111
286	45.566	163.795	101.36
287	45.566	163.795	98.585
288	42.655	167.190	101.53
289	42.655	167.190	98.930
290	45.358	158.717	101.22
291	45.358	158.717	98.098
292	40.30	175.9	100.30
293	40.30	182.0	100.30
299	50.07	148.544	96.921

GRID NUMBER	X_F	Y_F	Z_F
300	48.102	150.718	99.393
301	48.102	150.718	96.922
302	45.15	153.978	100.88
303	45.15	153.978	97.688
304	42.655	156.357	101.47
305	42.655	156.357	98.085
306	42.655	161.421	101.58
307	42.655	161.421	98.505
308	42.655	151.677	101.18
309	42.655	151.677	97.648
310	41.477	150.590	101.32
311	41.477	150.590	97.629
312	41.477	155.328	101.58
313	41.477	155.328	98.057
314	41.477	159.50	101.67
315	41.477	159.50	98.472
316	41.477	166.295	101.29
317	41.477	166.295	98.895
319	45.65	143.686	96.989
320	43.414	146.117	99.912
321	43.414	146.117	96.973
322	41.477	172.50	101.41
323	41.477	172.50	99.267
324	41.477	160.460	101.66
325	41.477	160.460	98.48
330	40.3	137.384	97.10
331	40.3	143.06	100.31
332	40.3	143.06	97.0
333	40.3	149.504	101.47

TABLE 6a. CONCLUDED

GRID NUMBER	X_F	Y_F	Z_F
334	40.3	149.504	97.61
335	40.3	154.30	101.70
336	40.3	154.30	98.03
337	40.3	159.50	101.77
338	40.3	159.50	98.44
339	40.3	165.40	101.68
340	40.3	165.40	98.86
341	42.655	172.50	101.43
342	42.655	172.50	99.284
343	40.3	172.50	101.40
344	40.3	172.50	99.25

TABLE 6b. CANARD GRID POINTS USED IN NASTRAN MODEL (COORDINATES IN INCHES)

GRID NUMBER	X_F	Y_F	Z_F
1305	11.16	58.593	106.08
1307	11.32	58.593	104.43
1401	9.815	45.10	103.645
1404	12.355	68.586	104.935
1405	12.09	68.586	106.625
1406	13.003	78.044	106.648
1407	13.415	78.448	105.514
1408	13.403	80.135	106.135
1409	14.116	86.986	106.300
1410	14.839	93.690	106.386
1415	16.703	56.227	105.264
1416	21.832	63.890	107.050
1417	16.572	65.585	108.005
1418	17.067	66.232	106.645
1419	16.481	71.031	108.256
1420	17.018	71.678	106.781
1421	16.506	75.705	108.187
1422	17.008	76.266	106.808
1423	16.603	81.572	107.920
1424	16.993	81.954	106.851
1425	17.995	90.366	107.725
1430	23.840	66.893	107.820
1431	18.771	68.457	108.801
1432	19.248	69.080	107.490
1434	21.090	71.486	109.637
1435	21.547	72.083	108.381
1436	20.160	77.665	109.575
1437	20.653	78.228	108.224
1440	20.841	87.424	108.832
1450	25.950	70.037	108.651

GRID NUMBER	X_F	Y_F	Z_F
1451	28.005	73.022	109.631
1452	28.005	73.022	109.631
1453	23.409	74.516	110.472
1454	23.846	75.086	109.272
1460	31.743	78.473	111.378
1461	27.651	80.056	111.884
1462	28.071	80.605	110.730
1463	24.695	82.849	111.168
1464	25.147	83.365	109.927
1465	21.498	86.368	109.671
1466	21.857	86.720	108.684
1470	34.942	83.179	112.816
1472	31.277	84.793	113.041
1473	31.689	85.331	111.911
1474	28.580	87.290	112.452
1475	29.019	87.791	111.248
1476	25.651	90.438	111.194
1477	25.991	90.772	110.259
1478	24.992	91.492	110.360
1479	22.391	94.196	109.324
1480	19.469	97.220	108.177
1484	38.210	88.027	114.062
1485	38.210	88.027	114.062
1486	34.905	89.532	114.195
1487	35.302	90.050	113.104
1488	32.459	91.723	113.756
1489	32.880	92.206	112.597
1490	29.776	94.481	112.793
1491	30.125	94.823	111.835
1492	29.104	95.522	111.997

TABLE 6b. CONCLUDED

GRID NUMBER	X_F	Y_F	Z_F
1493	26.763	98.005	110.990
1494	24.112	100.76	109.933
1500	41.485	92.894	115.291
1501	38.499	94.228	115.440
1502	38.857	94.695	114.456
1503	36.329	96.147	115.082
1504	36.722	96.597	114.002
1505	33.908	98.530	114.376
1506	34.259	98.875	113.410
1507	33.222	99.558	113.617
1508	31.095	101.77	112.766
1509	28.783	104.32	111.613
1510	33.219	103.62	113.626
1511	33.337	107.79	113.301
1512	33.939	103.40	114.291
1513	34.171	103.60	113.654
1520	45.273	98.529	116.751
1521	42.668	99.673	116.893
1522	42.979	100.07	116.038
1523	40.814	101.27	116.640
1524	41.155	101.66	115.702
1525	38.738	103.26	116.118
1526	39.055	103.57	115.246
1527	36.474	105.61	115.260
1528	36.700	105.81	114.640
1529	34.183	108.43	113.620
1530	45.273	98.529	116.751
1540	47.724	102.16	117.801
1541	45.537	103.42	117.867
1542	45.791	103.75	117.169

GRID NUMBER	X_F	Y_F	Z_F
1543	43.912	104.816	117.695
1544	44.217	105.165	116.856
1545	42.082	106.541	117.277
1546	42.366	106.820	116.496
1547	39.986	108.676	116.551
1548	40.190	108.854	115.991
1549	37.879	111.257	115.074
1555	50.0	105.55	118.778
1556	48.390	107.147	118.714
1557	48.482	107.267	118.462
1558	47.038	108.390	118.613
1559	47.209	108.585	118.144
1560	45.447	109.838	118.386
1561	45.672	110.060	117.766
1562	43.507	111.744	117.818
1563	43.692	111.905	117.310
1564	41.573	114.075	116.532
1565	50.0	109.25	119.192
1566	50.0	111.775	119.417
1567	48.693	113.020	119.266
1568	48.758	113.083	119.088
1569	46.907	114.705	118.916
1570	47.013	114.797	118.625
1571	45.066	116.738	117.892
1572	50.0	114.300	119.619
1573	50.0	117.400	119.845
1574	50.0	120.50	119.756

TABLE 7a. OUTER WING TEST LOADS, PAD LOCATIONS AND MAGNITUDES

Pad No.	X_F, Cm (in.)	Y_F, Cm (in.)	Load, Newtons (lb)
1	109.98 (43.3)	370.33 (145.8)	889.64 (200.)
2	123.19 (48.5)	383.79 (151.1)	613.85 (138.)
3	135.38 (53.3)	396.49 (156.1)	613.85 (138.)
4	149.10 (58.7)	407.67 (160.5)	613.85 (138.)
5	160.27 (63.1)	419.1 (165.0)	524.89 (118.)
6	171.20 (67.4)	429.77 (169.2)	524.89 (118.)
7	182.63 (71.9)	441.2 (173.7)	524.89 (118.)
8	193.80 (76.3)	452.37 (178.1)	524.89 (118.)
9	204.98 (80.7)	463.55 (182.5)	524.89 (118.)
10	217.93 (85.8)	477.01 (187.8)	524.89 (118.)
11	111.25 (43.8)	396.75 (156.2)	644.99 (145.)
12	122.43 (48.2)	407.16 (160.3)	644.99 (145.)
13	133.86 (52.7)	417.07 (164.2)	644.99 (145.)
14	145.54 (57.3)	427.74 (168.4)	569.37 (128.)
15	157.23 (61.9)	438.4 (172.6)	569.37 (128.)
16	168.4 (66.3)	449.58 (177.0)	569.37 (128.)

TABLE 7a. CONTINUED

Pad No.	X_F, Cm (in.)	Y_F, Cm (in.)	Load, Newtons (lb)
17	180.34 (71.0)	460.25 (181.2)	489.3 (110.)
18	192.02 (75.6)	471.17 (185.5)	489.3 (110.)
19	203.71 (80.2)	481.84 (189.7)	489.3 (110.)
20	108.97 (42.9)	421.64 (166.0)	133.45 (30.)
21	120.4 (47.4)	438.66 (172.7)	133.45 (30.)
22	134.62 (53.0)	449.07 (176.8)	133.45 (30.)
23	149.10 (58.7)	459.49 (180.9)	133.45 (30.)
24	163.32 (64.3)	469.9 (185.0)	222.41 (50.)
25	177.8 (70.0)	480.06 (189.0)	222.41 (50.)
26	192.02 (75.6)	490.73 (193.2)	222.41 (50.)
27	206.5 (81.3)	501.14 (197.3)	222.41 (50.)
28	222.76 (87.7)	492.76 (194.0)	360.31 (81.)
29	221.74 (87.3)	508.51 (200.2)	271.34 (61.)
30	221.74 (87.3)	529.84 (208.61)	271.34 (61.)
31	127.51 (50.2)	474.73 (186.9)	177.93 (40.)

TABLE 7a. CONCLUDED

Pad No.	X_F, Cm (in.)	Y_F, Cm (in.)	Load, Newtons (lb)
32	143.26 (56.4)	481.84 (189.7)	177.93 (40.)
33	160.78 (63.3)	491.74 (193.6)	177.93 (40.)
34	175.77 (69.2)	501.65 (197.5)	177.93 (40.)
35	190.25 (74.9)	512.06 (201.6)	177.93 (40.)
36	204.72 (80.6)	521.97 (205.5)	177.93 (40.)

TABLE 7b. CANARD TEST LOADS, PAD LOCATIONS AND MAGNITUDES

Pad No.	X_C, Cm (in.)	Y_C, Cm (in.)	Load, Newtons (lb)
1	32.51 (12.8)	137.67 (54.2)	489.3 (110.)
2	39.37 (15.5)	153.67 (60.5)	934.13 (210.)
3	49.53 (19.5)	169.16 (66.6)	934.13 (210.)
4	60.2 (23.7)	184.15 (72.5)	934.13 (210.)
5	70.61 (27.8)	199.64 (78.6)	934.13 (210.)
6	81.53 (32.1)	212.34 (83.6)	667.23 (150.)
7	90.93 (35.8)	226.06 (89.0)	667.23 (150.)
8	100.33 (39.5)	239.52 (94.3)	667.23 (150.)
9	108.97 (42.9)	252.73 (99.5)	644.99 (145.)
10	118.36 (46.6)	266.19 (104.8)	644.99 (145.)
11	37.59 (14.8)	183.64 (72.3)	444.82 (100.)
12	47.75 (18.8)	204.98 (80.7)	244.65 (55.)
13	60.45 (23.8)	217.93 (85.8)	244.65 (55.)
14	72.9 (28.7)	230.38 (90.7)	244.65 (55.)
15	85.85 (33.8)	243.08 (95.7)	244.65 (55.)

TABLE 7b. CONCLUDED

Pad No.	X_c, Cm (in.)	Y_c, Cm (in.)	Load, Newtons (lb)
16	44.7 (17.6)	228.6 (90.0)	222.41 (50.)
17	60.45 (23.8)	242.06 (95.3)	222.41 (50.)
18	76.2 (30.0)	255.52 (100.6)	222.41 (50.)
19	97.03 (38.2)	272.03 (107.1)	266.89 (60.)
20	109.73 (43.2)	283.72 (111.7)	266.89 (60.)

TABLE 8. DEFLECTION TRANSDUCER LOCATIONS AND VERTICAL DISPLACEMENT MEASUREMENTS FOR THE VERIFICATION LOAD TEST

Nominal Grid No.	Location	Coordinates			Measured Vertical Displacement, cm (in.)
		X_F, cm (in.)	Y_F, cm (in.)	Z_F, cm (in.)	
25	LH wing	225.6 (88.8)	478.5 (188.4)	248.2 (97.7)	11.24 (4.43)
27	LH wing	224.7 (88.4)	488.8 (192.4)	251.0 (98.8)	11.61 (4.57)
31	LH wing	223.5 (88.0)	522.0 (205.5)	253.8 (99.9)	13.83 (5.45)
33	LH wing	224.5 (88.4)	545.8 (214.9)	253.2 (99.7)	15.54 (6.12)
71	LH wing	203.6 (80.2)	531.6 (209.3)	253.7 (99.87)	12.92 (5.09)
75	LH wing	210.3 (82.8)	508.6 (200.2)	252.2 (99.3)	11.33 (4.46)
95	LH wing	212.8 (83.8)	482.8 (190.1)	249.2 (98.1)	10.16 (4.00)
103	LH wing	199.0 (78.4)	501.8 (197.6)	252.5 (99.4)	9.86 (3.88)
106	LH wing	185.4 (73.0)	519.0 (204.4)	253.8 (99.9)	10.39 (4.09)
140	LH wing	206.2 (81.2)	457.8 (180.2)	247.9 (97.6)	8.02 (3.16)
144	LH wing	197.9 (77.9)	465.6 (183.3)	249.2 (98.1)	7.80 (3.07)
152	LH wing	179.2 (70.6)	488.2 (192.2)	253.0 (99.6)	7.08 (2.79)

TABLE 8. CONTINUED

Nominal Grid No.	Location	Coordinates			Measured Vertical Displacement, cm (in.)
		$X_{F'}$ cm (in.)	$Y_{F'}$ cm (in.)	$Z_{F'}$ cm (in.)	
155	LH wing	168.4 (66.3)	506.7 (199.5)	254.0 (100.0)	8.09 (3.19)
186	LH wing	186.2 (73.3)	438.7 (172.7)	247.6 (97.5)	6.48 (2.55)
193	LH wing	175.5 (69.1)	448.4 (176.6)	248.9 (98.0)	5.04 (1.98)
201	LH wing	156.8 (61.8)	472.2 (185.9)	254.2 (99.6)	5.12 (1.83)
228	LH wing	143.6 (56.6)	492.2 (193.8)	254.2 (100.1)	5.12 (2.02)
239	LH wing	164.3 (64.7)	416.6 (164.0)	248.2 (97.7)	4.33 (1.70)
243	LH wing	153.7 (60.5)	426.2 (167.8)	248.4 (97.8)	3.17 (1.25)
251	LH wing	131.2 (51.6)	455.4 (179.3)	252.8 (99.53)	2.42 (.095)
254	LH wing	119.9 (47.2)	483.2 (190.2)	254.6 (100.2)	3.72 (1.47)
274	LH wing	104.6 (41.2)	477.5 (188.0)	254.8 (100.3)	2.89 (1.14)
278	LH wing	114.6 (45.1)	444.2 (174.9)	252.5 (99.4)	1.45 (0.57)
299	LH wing	127.5 (50.2)	379.1 (149.2)	246.1 (96.9)	2.35 (0.92)

TABLE 8. CONTINUED

Nominal Grid No.	Location	Coordinates $X_{F'}$ cm (in.)	Coordinates $Y_{F'}$ cm (in.)	Coordinates $Z_{F'}$ cm (in.)	Measured Vertical Displacement, cm (in.)
303	LH wing	115.6 (45.5)	390.4 (153.7)	248.2 (97.7)	1.18 (0.46)
423	LH wing	86.4 (34.0)	438.2 (172.5)	251.9 (99.2)	0.47 (0.19)
436	LH wing	86.4 (34.0)	405.1 (159.5)	250.1 (98.5)	0.42 (0.17)
440	LH wing	86.4 (34.0)	357.9 (140.9)	247.0 (97.3)	0.39 (0.16)
464	LH wing	60.3 (23.8)	438.2 (172.5)	251.0 (98.8)	0.09 (0.03)
466	LH wing	60.3 (23.8)	405.1 (159.5)	249.9 (98.4)	0.05 (0.02)
470	LH wing	60.3 (23.8)	357.9 (140.9)	247.9 (97.6)	0.13 (0.05)
1555	LH can	127.0 (50.0)	268.1 (105.6)	301.8 (118.8)	7.62 (3.00)
1565	LH can	127.0 (50.0)	277.5 (109.2)	302.8 (119.2)	8.11 (3.19)
1572	LH can	127.0 (50.0)	290.3 (114.3)	303.8 (119.6)	8.70 (3.42)
1574	LH can	127.0 (50.0)	306.1 (120.5)	304.3 (119.8)	9.31 (3.66)
1568	LH can	123.8 (48.8)	287.2 (113.1)	302.5 (119.1)	8.41 (3.31)

TABLE 8. CONTINUED

Nominal Grid No.	Location	Coordinates X_F, cm (in.)	Coordinates Y_F, cm (in.)	Coordinates Z_F, cm (in.)	Measured Vertical Displacement, cm (in.)
1557	LH can	123.14 (48.5)	272.0 (107.1)	301.0 (118.5)	7.62 (3.00)
1561	LH can	116.0 (45.7)	279.6 (110.1)	299.2 (117.8)	7.45 (2.93)
1564	LH can	105.6 (41.6)	289.8 (114.1)	295.9 (116.5)	7.16 (2.82)
1522	LH can	109.2 (43.0)	253.2 (99.7)	294.6 (116.0)	5.92 (2.33)
1526	LH can	99.2 (39.1)	263.1 (103.6)	292.6 (115.2)	5.53 (2.18)
1529	LH can	86.8 (34.2)	275.4 (108.4)	288.5 (113.6)	5.31 (2.09)
1530	LH can	115.0 (45.3)	250.9 (98.8)	296.7 (116.8)	6.08 (2.40)
1511	LH can	84.7 (33.3)	273.7 (107.8)	287.8 (113.3)	5.19 (2.04)
1485	LH can	97.1 (38.2)	224.2 (88.2)	289.8 (114.1)	3.61 (1.42)
1487	LH can	89.7 (35.3)	228.1 (89.8)	287.3 (113.1)	3.36 (1.32)
1491	LH can	76.5 (30.1)	240.8 (94.8)	284.0 (111.8)	3.04 (1.20)
1494	LH can	61.2 (24.1)	255.9 (100.8)	279.2 (109.9)	3.90 (1.54)

TABLE 8. CONTINUED

Nominal Grid No.	Location	Coordinates			Measured Vertical Displacement, cm (in.)
		$X_{F'}$ cm (in.)	$Y_{F'}$ cm (in.)	$Z_{F'}$ cm (in.)	
1460	LH can	79.8 (31.7)	199.6 (78.6)	283.0 (111.4)	2.15 (0.85)
1464	LH can	71.3 (28.1)	204.0 (80.3)	281.2 (110.7)	1.78 (0.70)
1466	LH can	55.5 (21.9)	220.3 (86.7)	276.1 (108.7)	1.29 (0.51)
1410	LH can	37.7 (14.8)	238.0 (93.7)	270.3 (106.4)	2.56 (1.01)
1424	LH can	43.2 (17.0)	208.2 (82.0)	271.5 (106.9)	0.01 (0.00)
1416	LH can	55.4 (21.8)	162.2 (63.8)	272.0 (107.1)	1.21 (0.48)
1418	LH can	43.4 (17.1)	167.4 (65.9)	270.8 (106.6)	0.76 (0.30)
27	RH wing	-224.2 (-88.2)	493.0 (194.1)	251.0 (98.8)	12.11 (4.77)
31	RH wing	-224.8 (-88.5)	521.2 (205.2)	253.8 (99.9)	13.84 (5.45)
193	RH wing	-175.5 (-69.1)	448.4 (176.6)	248.8 (98.0)	5.27 (2.08)
201	RH wing	-156.8 (-61.8)	472.2 (185.9)	253.0 (99.6)	4.85 (1.91)
423	RH wing	-86.4 (-34.0)	438.2 (172.5)	251.9 (99.2)	0.65 (0.26)

TABLE 8. CONCLUDED

Nominal Grid No.	Location	Coordinates			Measured vertical Displacement, cm (in.)
		$X_{F'}$ cm (in.)	$Y_{F'}$ cm (in.)	$Z_{F'}$ cm (in.)	
440	RH wing	-86.4 (-34.0)	357.9 (140.9)	247.0 (97.3)	0.62 (0.25)
1565	RH can	-127.0 (-50.0)	277.5 (109.2)	302.8 (119.2)	8.32 (3.27)
1572	RH can	-127.0 (-50.0)	290.3 (114.3)	303.8 (119.6)	8.97 (3.53)
---	Fuselage	0	65.4 (-25.8)	262.4 (103.3)	0.96 (0.38)
1377	Fuselage	0	55.9 (22.0)	255.0 (100.4)	0.68 (0.27)
---	Fuselage	0	153.0 (60.2)	214.9 (84.6)	0.34 (0.13)
---	Fuselage	0	233.7 (92.0)	204.0 (80.3)	0.17 (0.07)
---	Fuselage	0	293.4 (115.5)	204.7 (80.6)	0.17 (0.07)
---	Fuselage	0	355.6 (140.0)	209.8 (82.6)	0.06 (0.02)
822	Fuselage	0	405.1 (159.5)	212.0 (83.4)	-0.03 (-0.01)
649	Fuselage	0	438.2 (172.5)	214.6 (84.5)	-0.01 (0)
617	Fuselage	0	489.0 (192.5)	218.9 (86.2)	-0.16 (-0.06)
583	Fuselage	0	551.2 (217.0)	224.4 (88.3)	-0.25 (0.10)

TABLE 9. NASTRAN PREDICTED VERTICAL DISPLACEMENT UNDER PARTIAL 8g LOAD DISTRIBUTION

Model grid number	Predicted vertical displacement cm (in)
25	10.92 (4.30)
27	12.42 (4.89)
31	14.83 (5.84)
33	16.94 (6.67)
71	12.37 (4.87)
75	11.76 (4.63)
95	9.60 (3.78)
103	9.55 (3.76)
106	9.35 (3.68)
140	6.78 (2.67)
144	6.76 (2.66)
152	6.76 (2.66)
155	7.71 (2.64)
186	3.81 (1.50)

Model grid number	Predicted vertical displacement cm (in)
193	3.96 (1.56)
201	3.81 (1.50)
228	3.20 (1.26)
239	1.83 (0.72)
243	1.93 (0.76)
251	1.70 (0.67)
254	1.83 (0.72)
274	0.99 (0.39)
278	0.97 (0.38)
299	0.76 (0.30)
303	0.69 (0.27)
423	0.41 (0.16)
436	0.38 (0.15)
440	0.30 (0.12)

TABLE 9. CONCLUDED

Model grid number	Predicted vertical displacement cm (in)
464	0.13 (0.05)
466	0.13 (0.05)
470	0.15 (0.06)
1555	6.48 (2.55)
1565	7.06 (2.78)
1572	7.85 (3.09)
1574	8.79 (3.49)
1568	7.49 (2.95)
1557	6.55 (2.58)
1561	6.60 (2.60)
1564	6.65 (2.62)
1526	4.70 (1.85)
1526	4.70 (1.85)
1529	4.78 (1.88)

Model grid number	Predicted vertical displacement cm (in)
1530	4.75 (1.87)
1511	3.76 (1.48)
1485	2.51 (0.99)
1487	2.44 (0.96)
1491	2.36 (0.93)
1494	2.84 (1.12)
1460	1.24 (0.49)
1462	1.12 (0.44)
1466	0.86 (0.34)
1410	1.73 (0.68)
1424	0.46 (0.18)
1416	0.74 (0.29)
1418	0.56 (0.22)

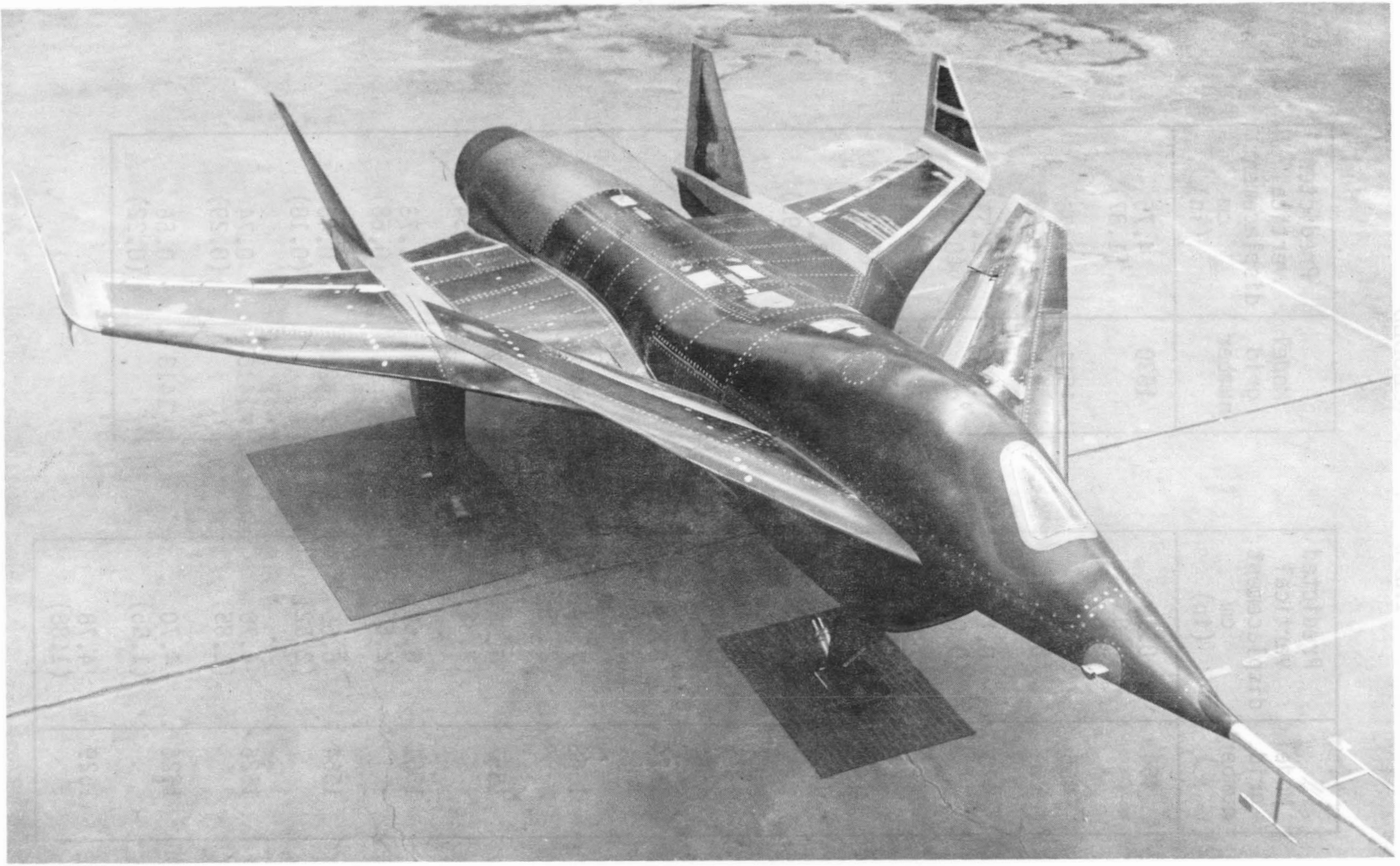

Figure 1. HiMAT aircraft.

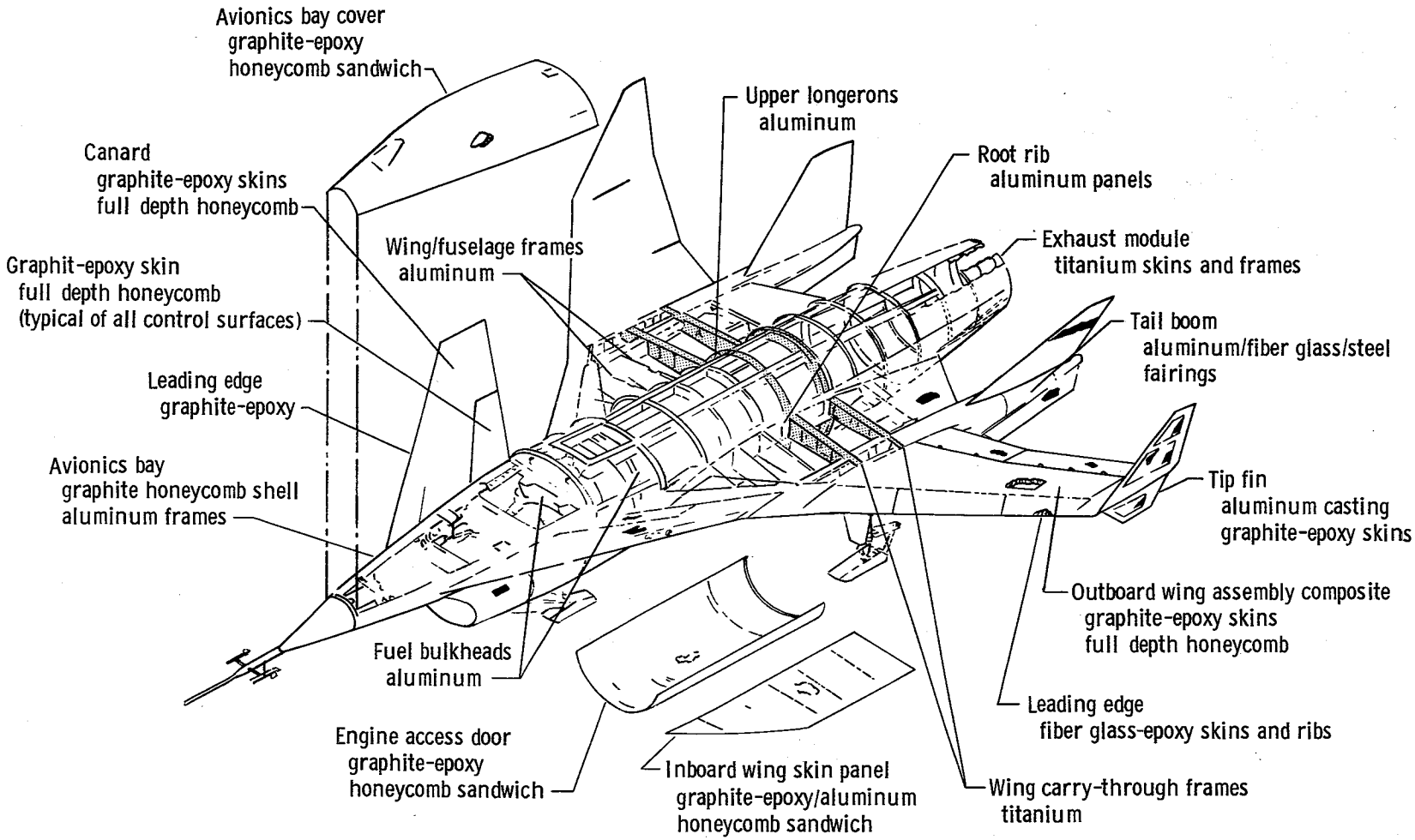

Figure 2. HiMAT structural configuration.

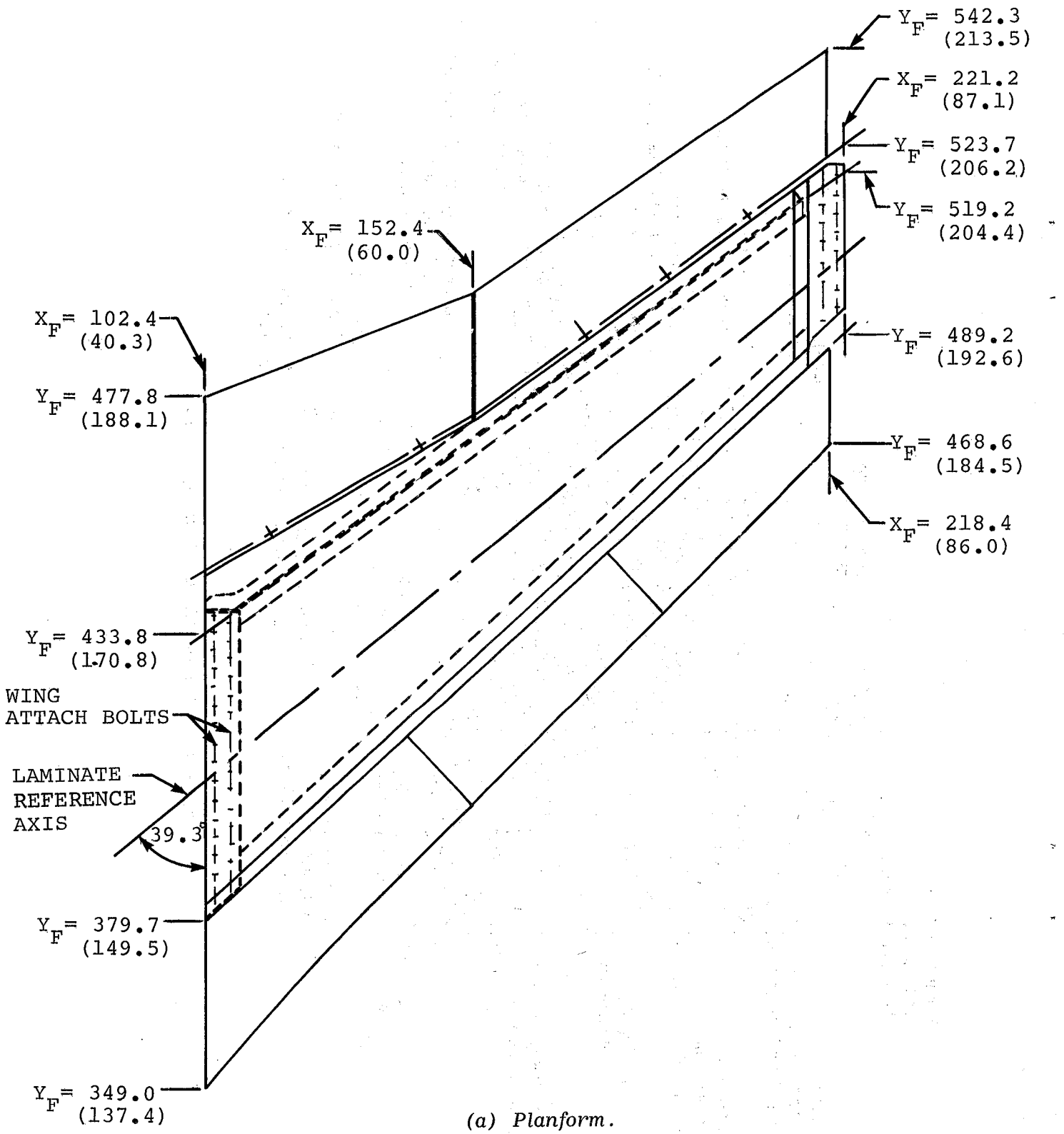

(a) Planform.

Figure 3. HiMAT tailored composite outer wing. Dimensions in centimeters (inches).

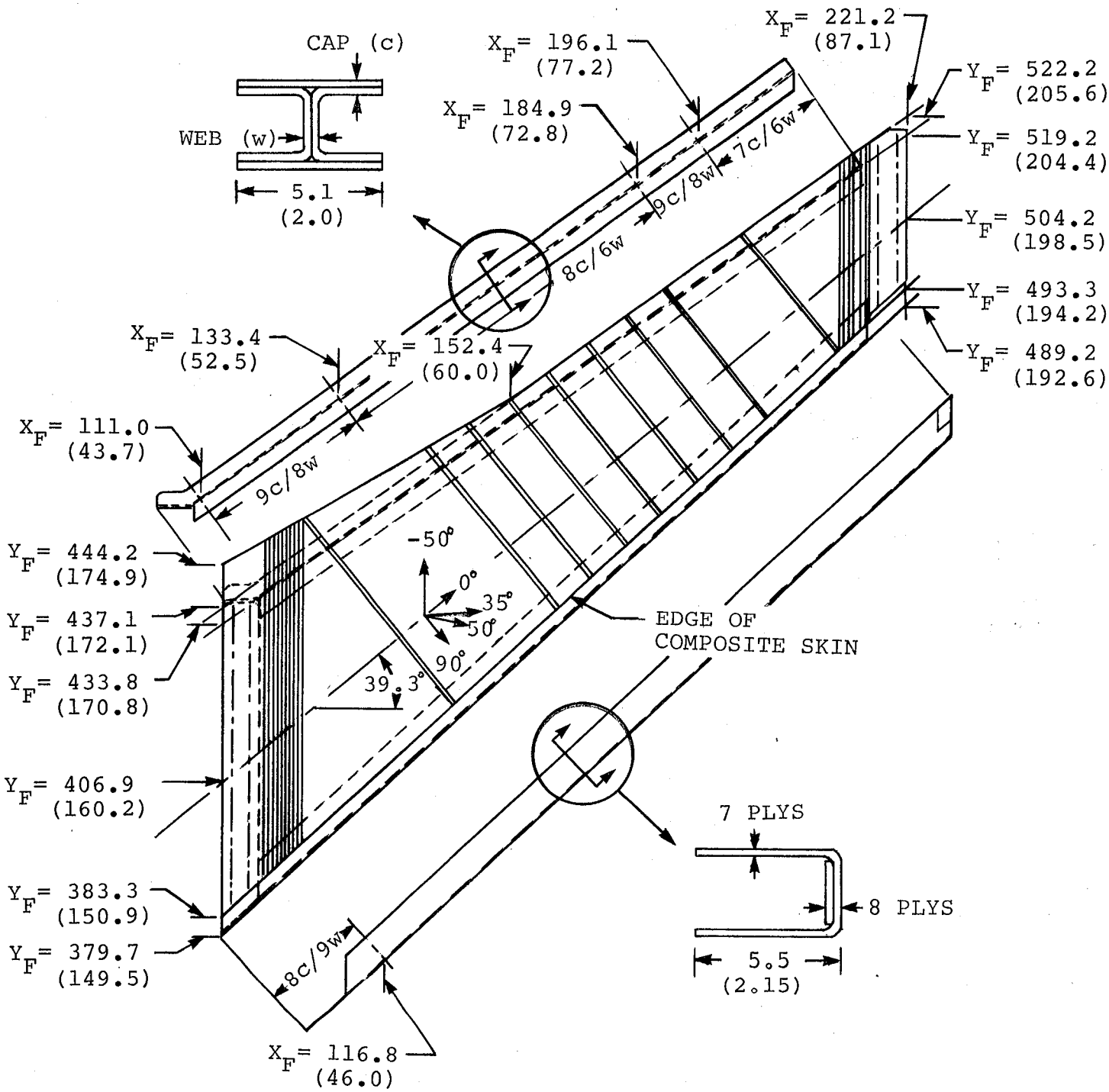

(b) Structural box.

Figure 3. Continued.

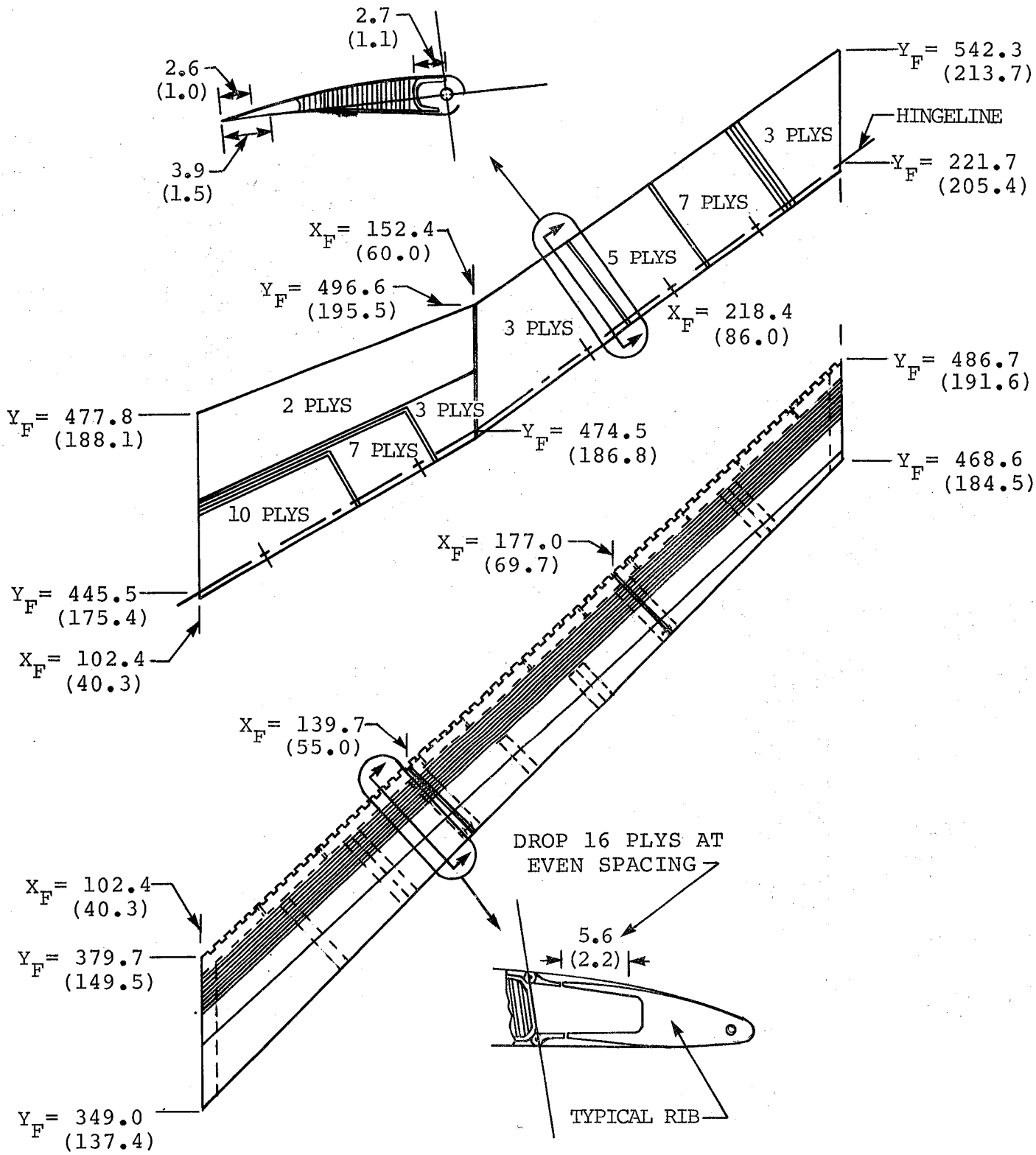

(c) Aileron, elevon, and leading edge structure.

Figure 3. Concluded.

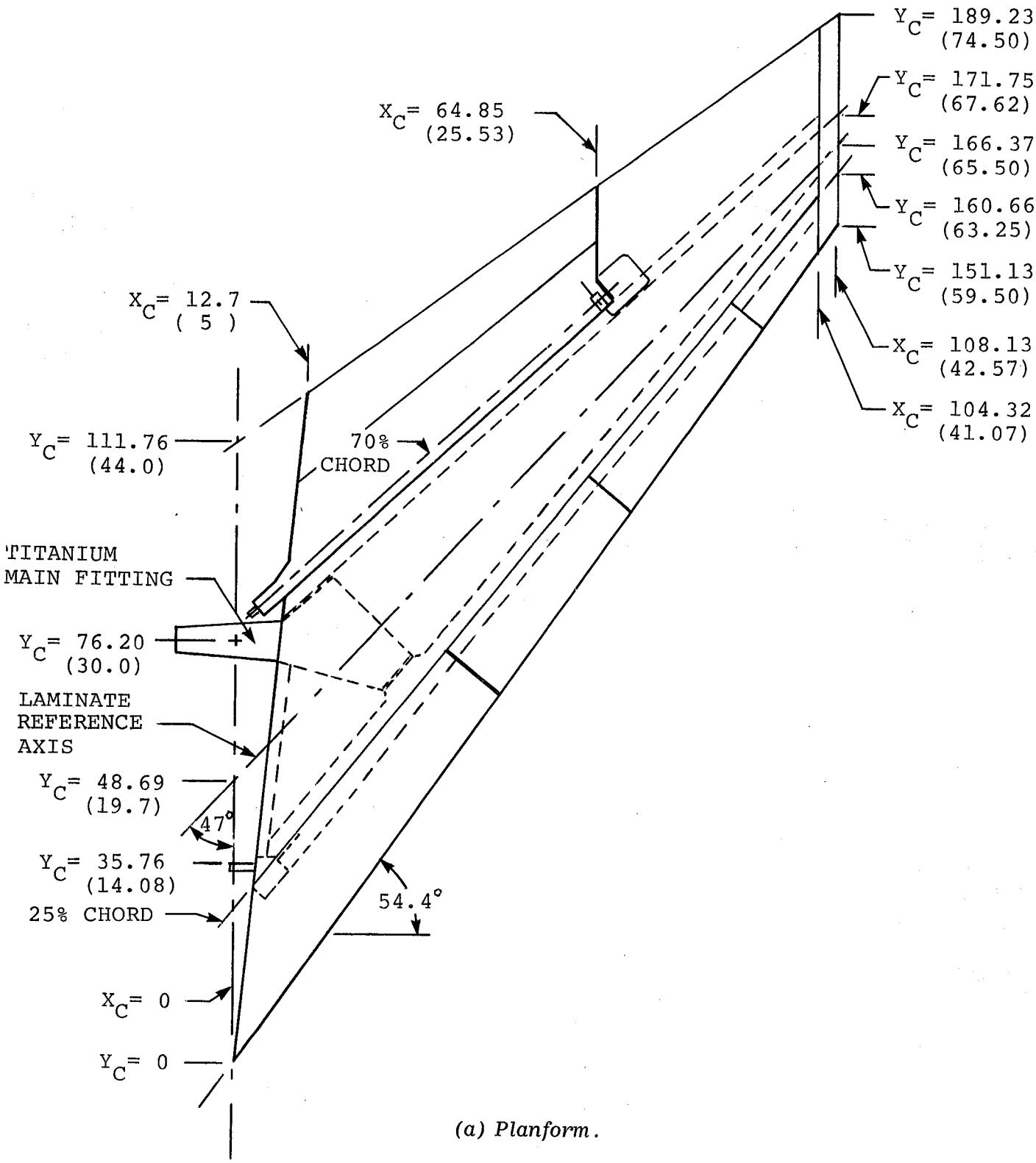

(a) Planform.

Figure 4. HiMAT tailored composite canard. Dimensions are in centimeters (inches).

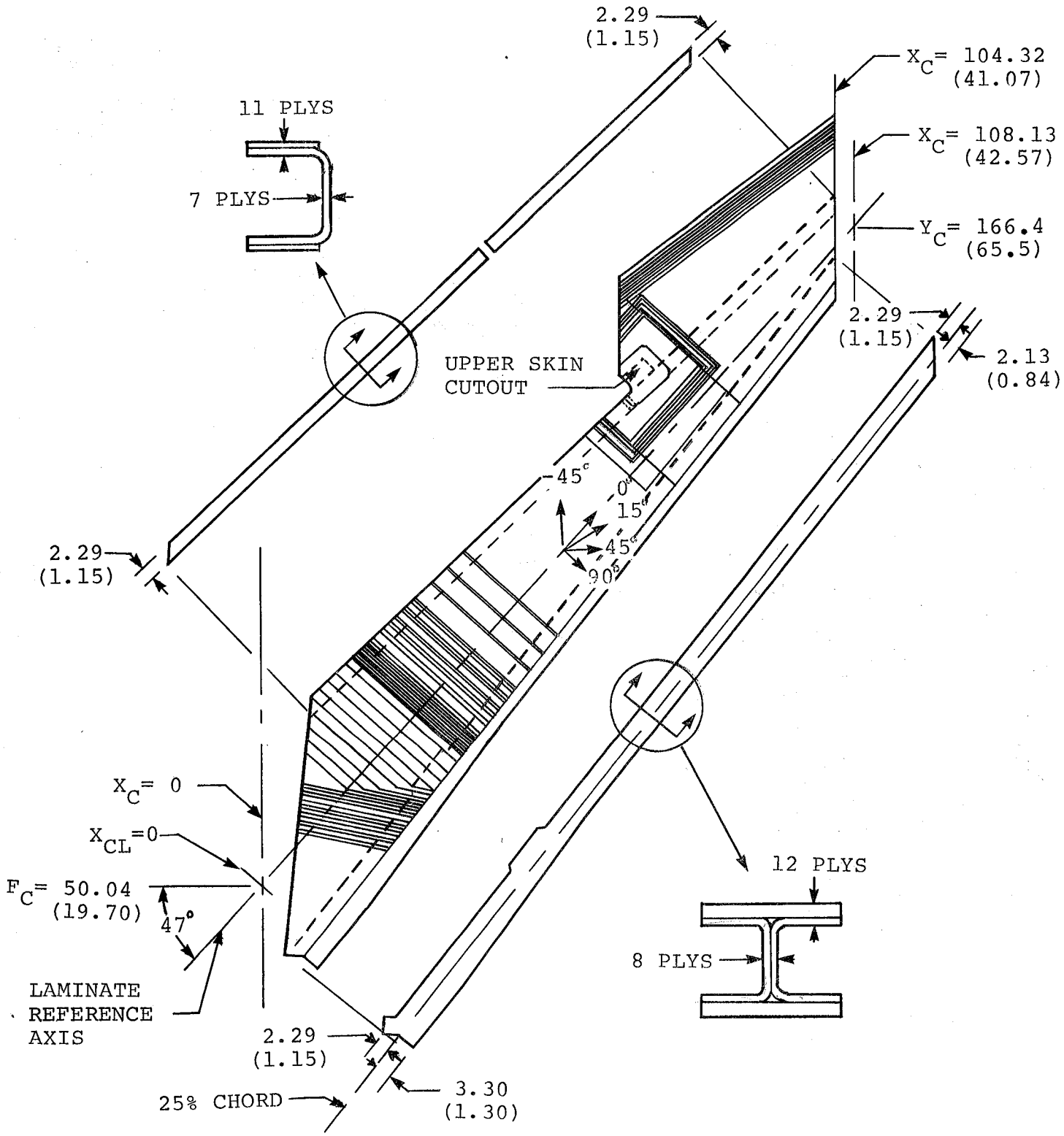

(b) Structural box.

Figure 4. Continued.

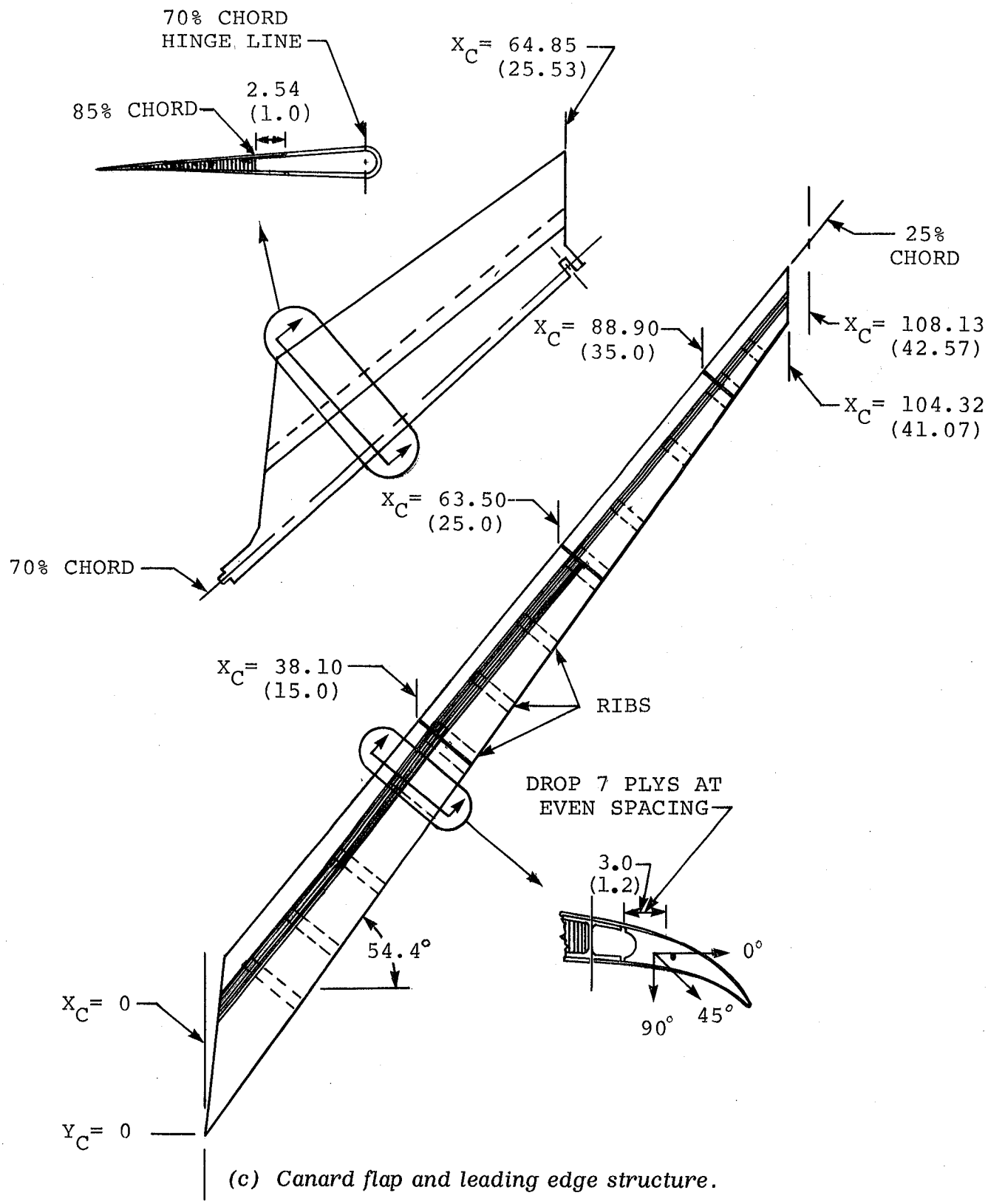

(c) Canard flap and leading edge structure.

Figure 4. Concluded.

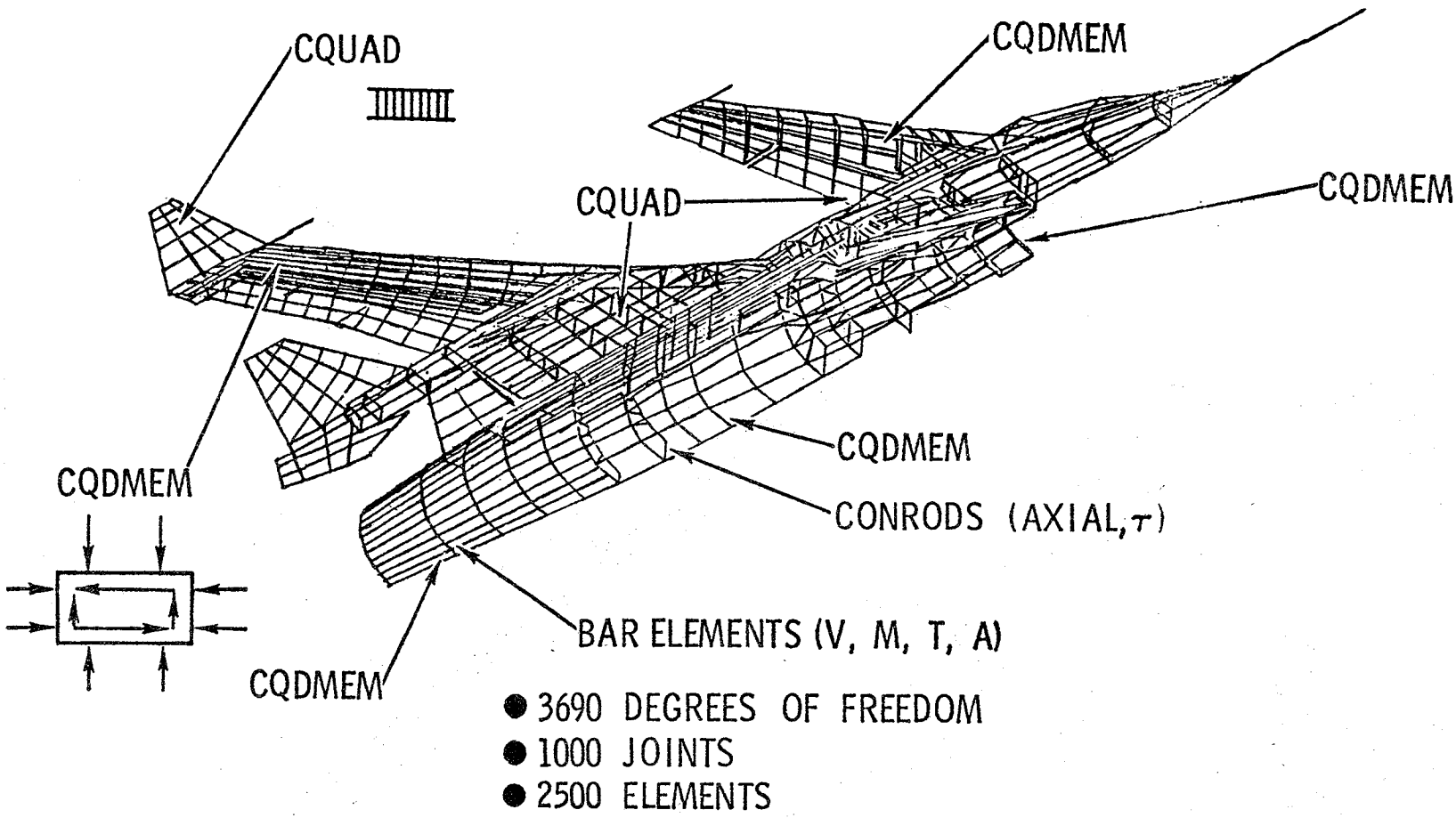

Figure 5. NASTRAN structural model.

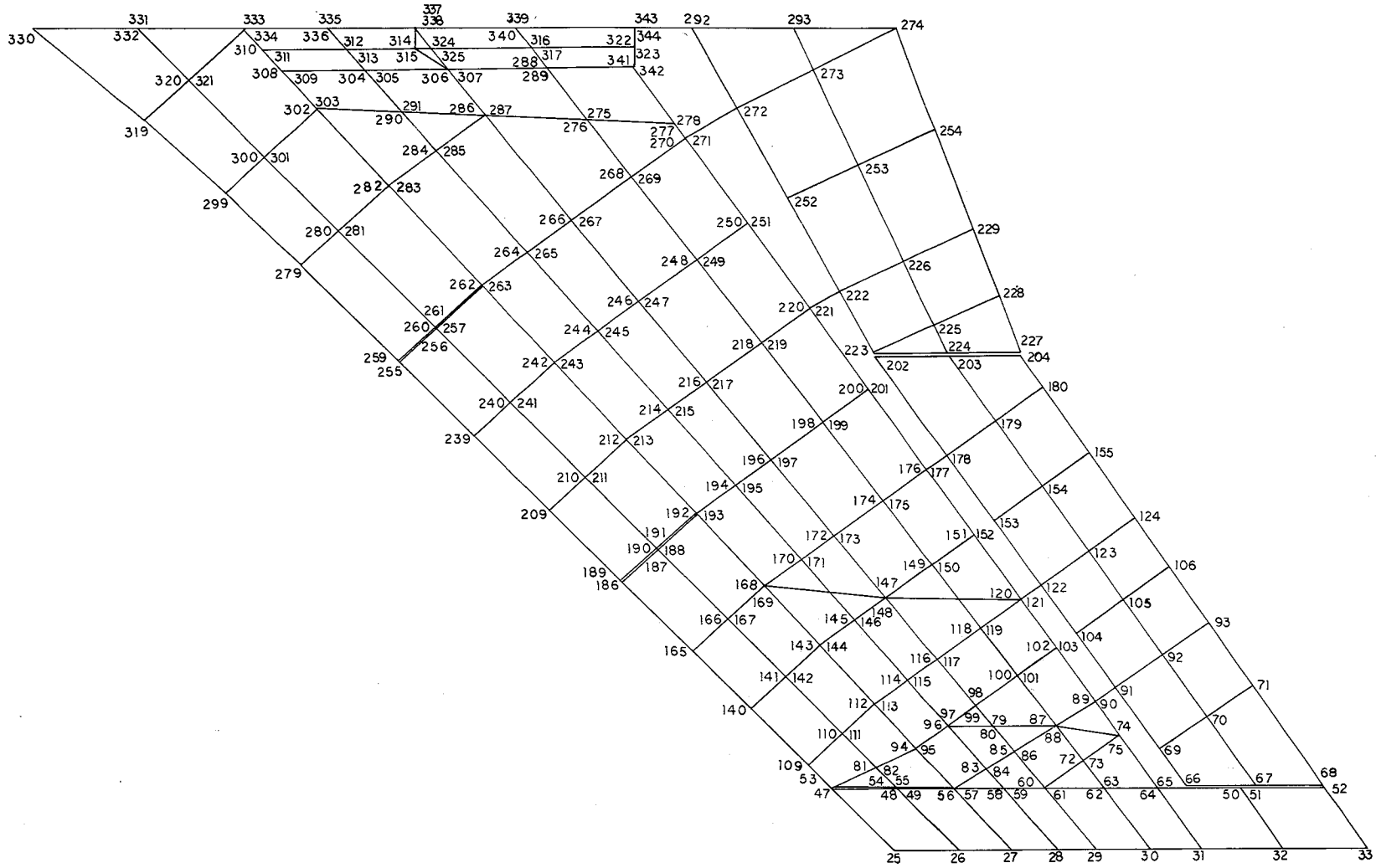

(a) Outer wing.

Figure 6. NASTRAN model.

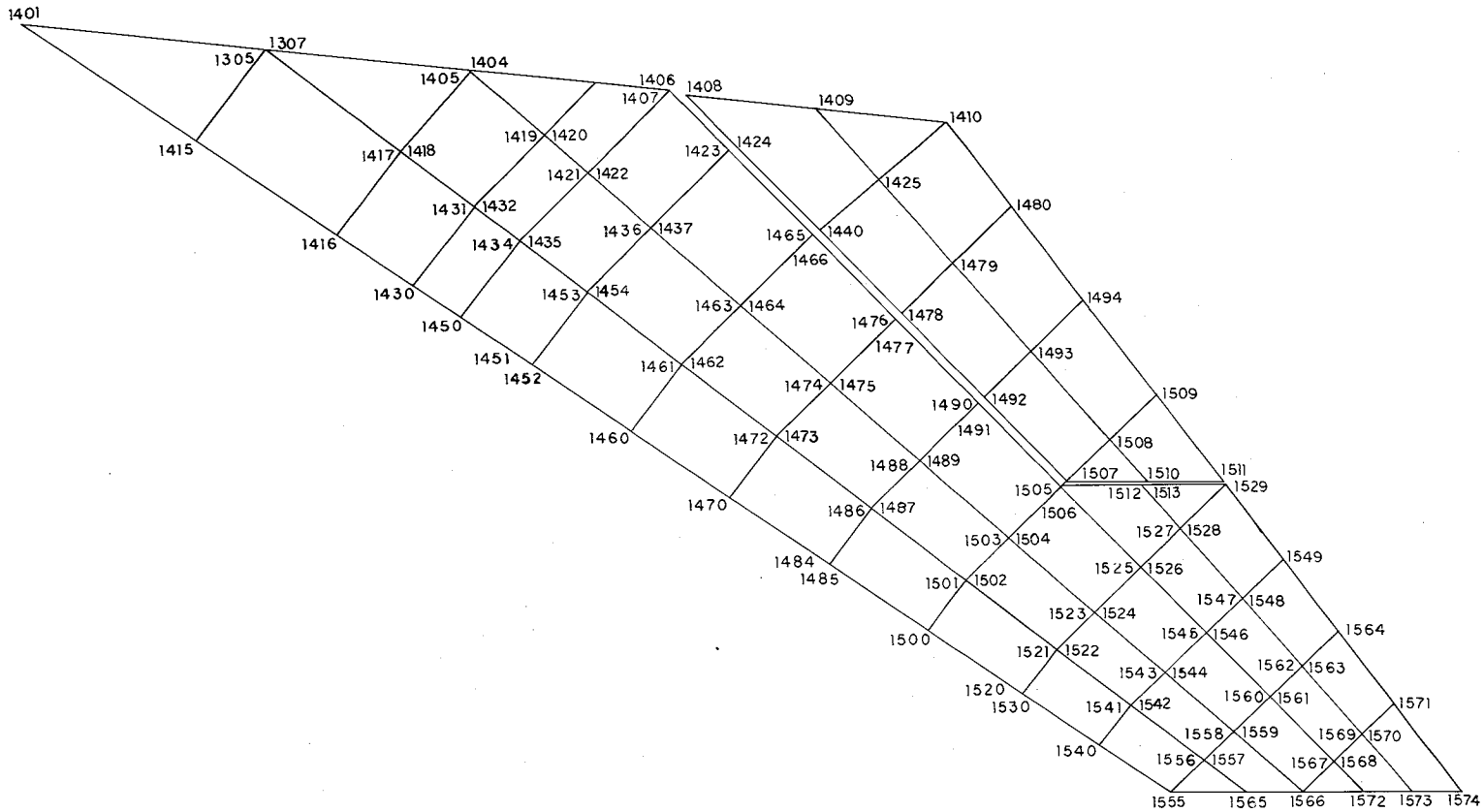

(b) Canard.

Figure 6. Concluded.

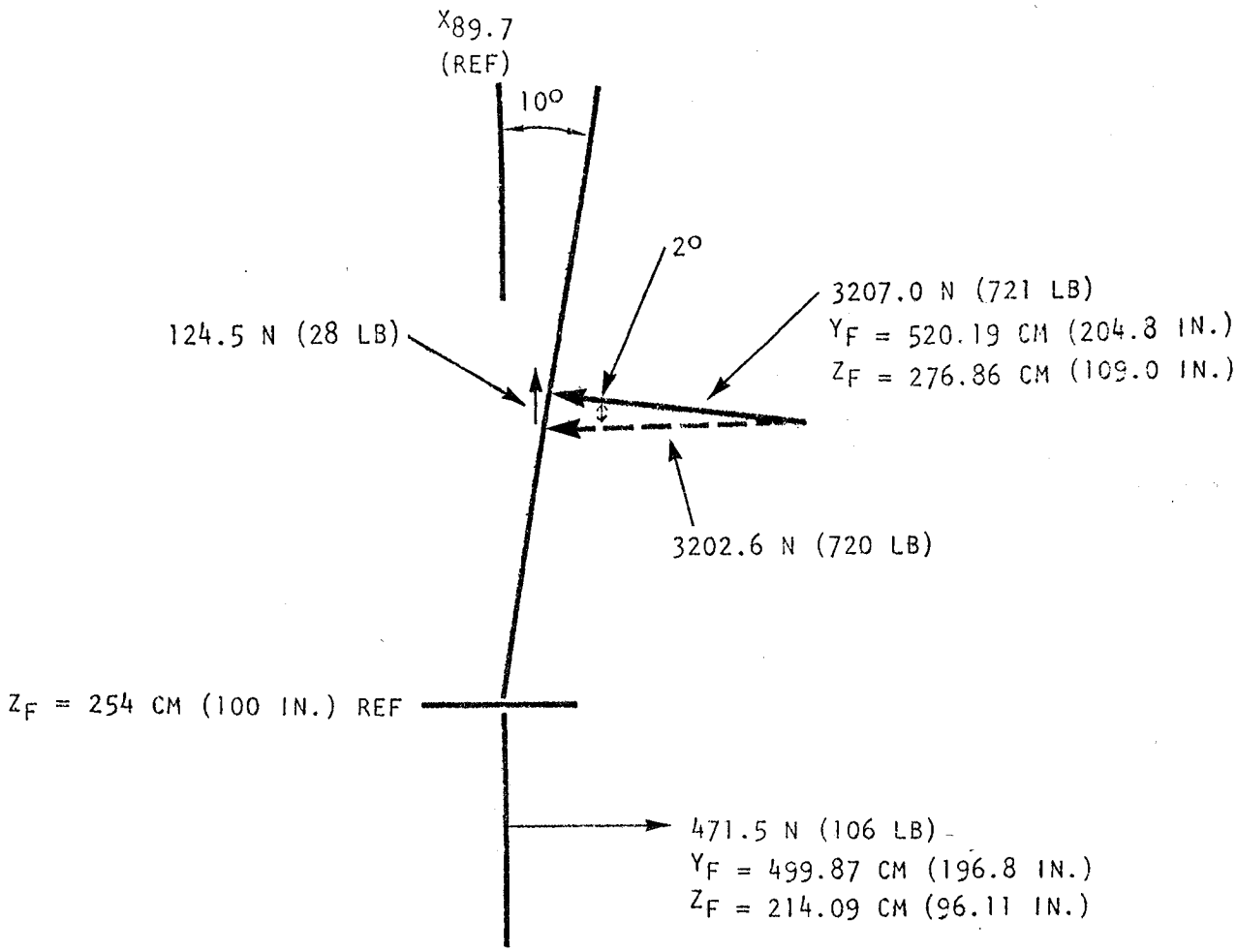

(a) Wing tip-fin.

Figure 7. Load pad locations. View looking aft on the left-hand side.

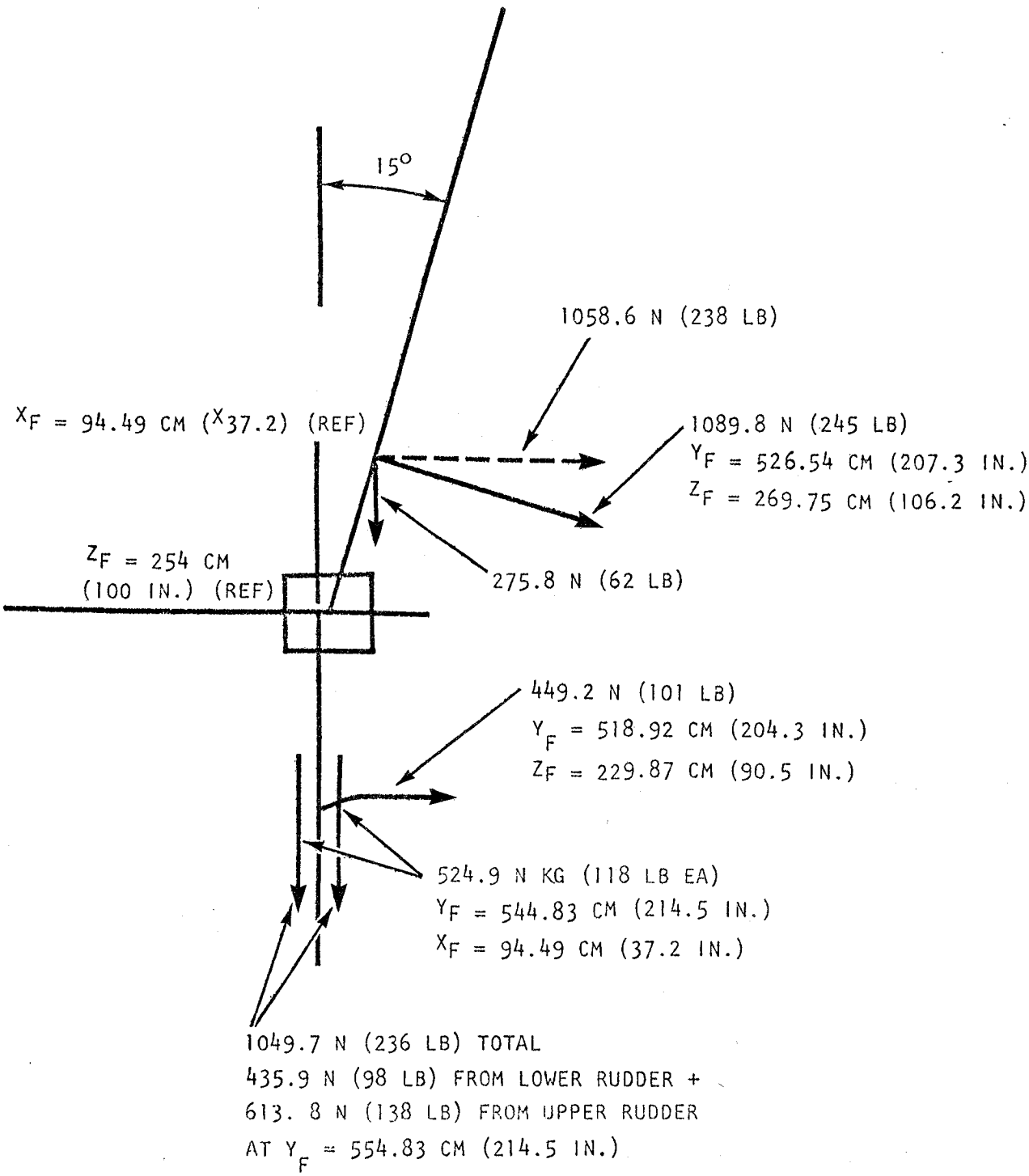

(b) Rudder.

Figure 7. Concluded.

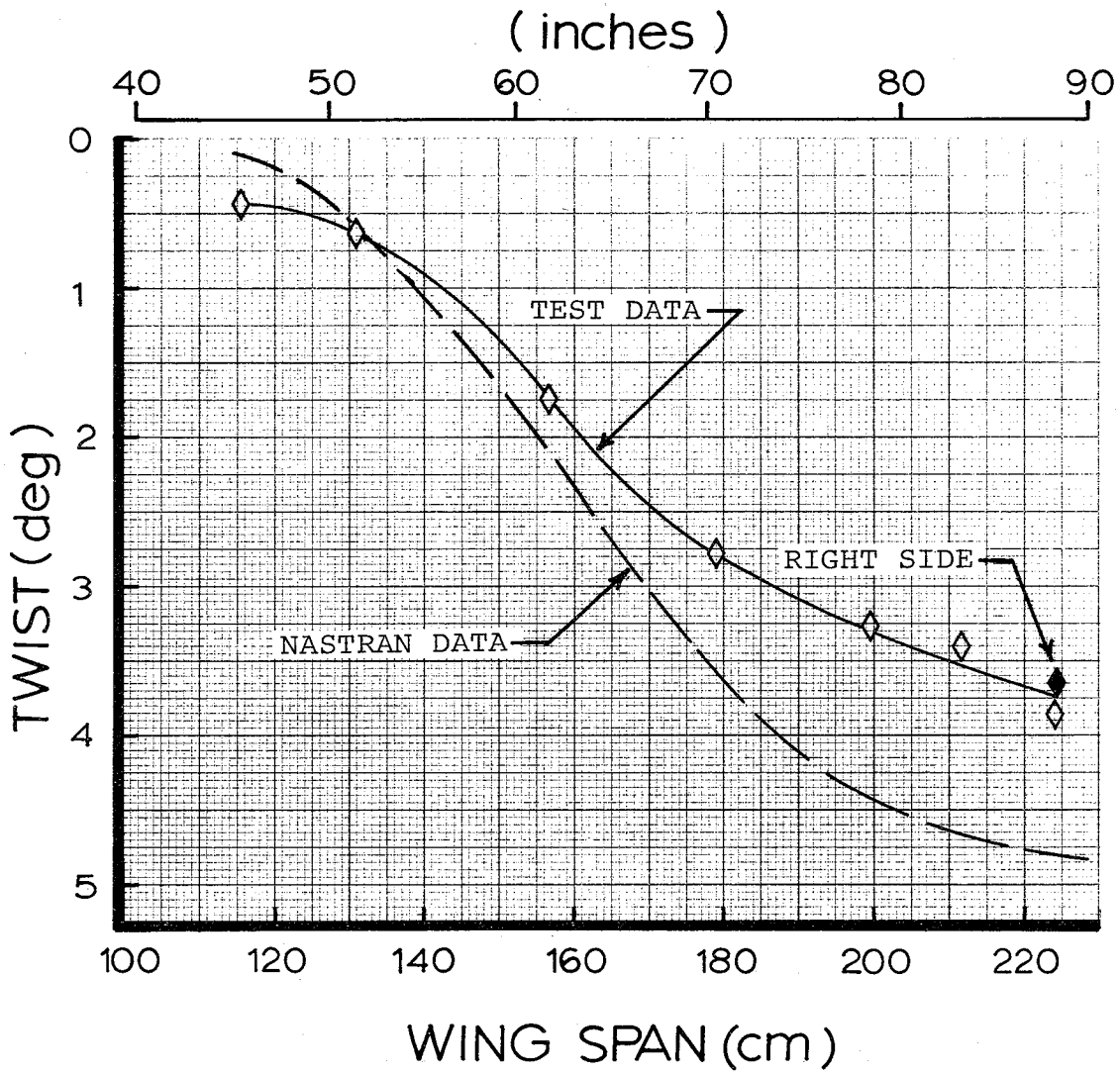

(a) Outer wing left side (except as noted).

Figure 8. Verification test twist distribution measured between front and rear spars.

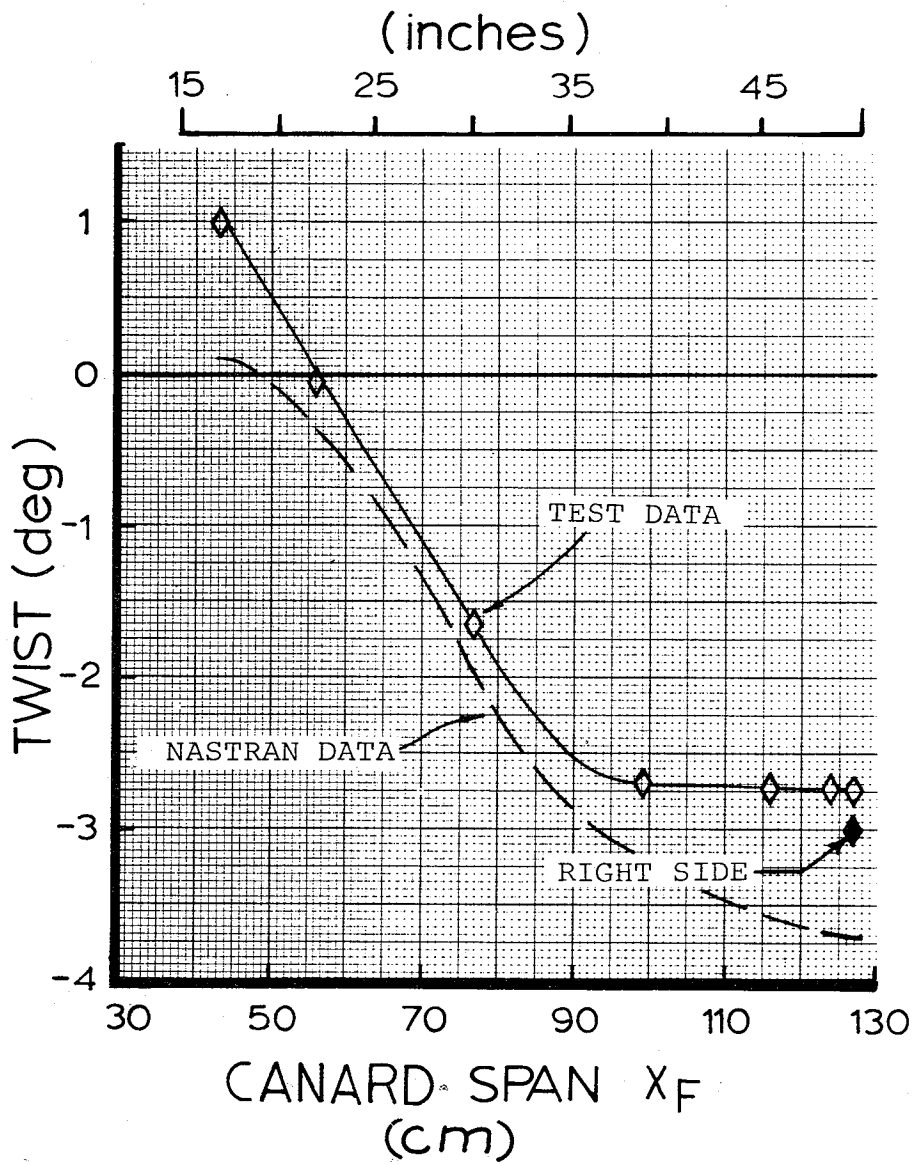

(b) Canard, left side (except as noted).

Figure 8. Concluded.

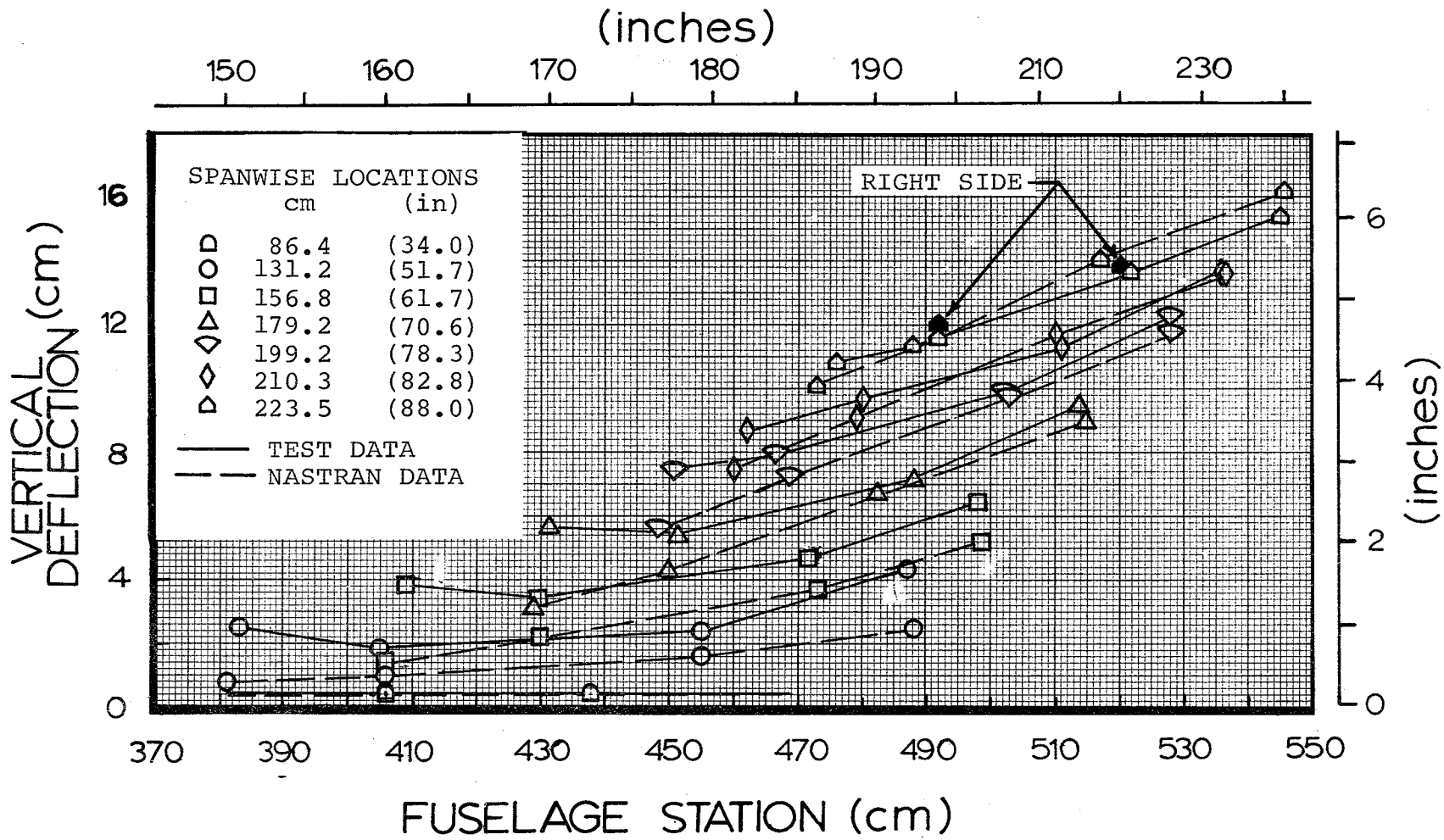

(a) Outer wing, left side (except as noted).

Figure 9. Verfication-test vertical displacement for the leading edge, front spar, rear spar, and trailing edge at several span locations.

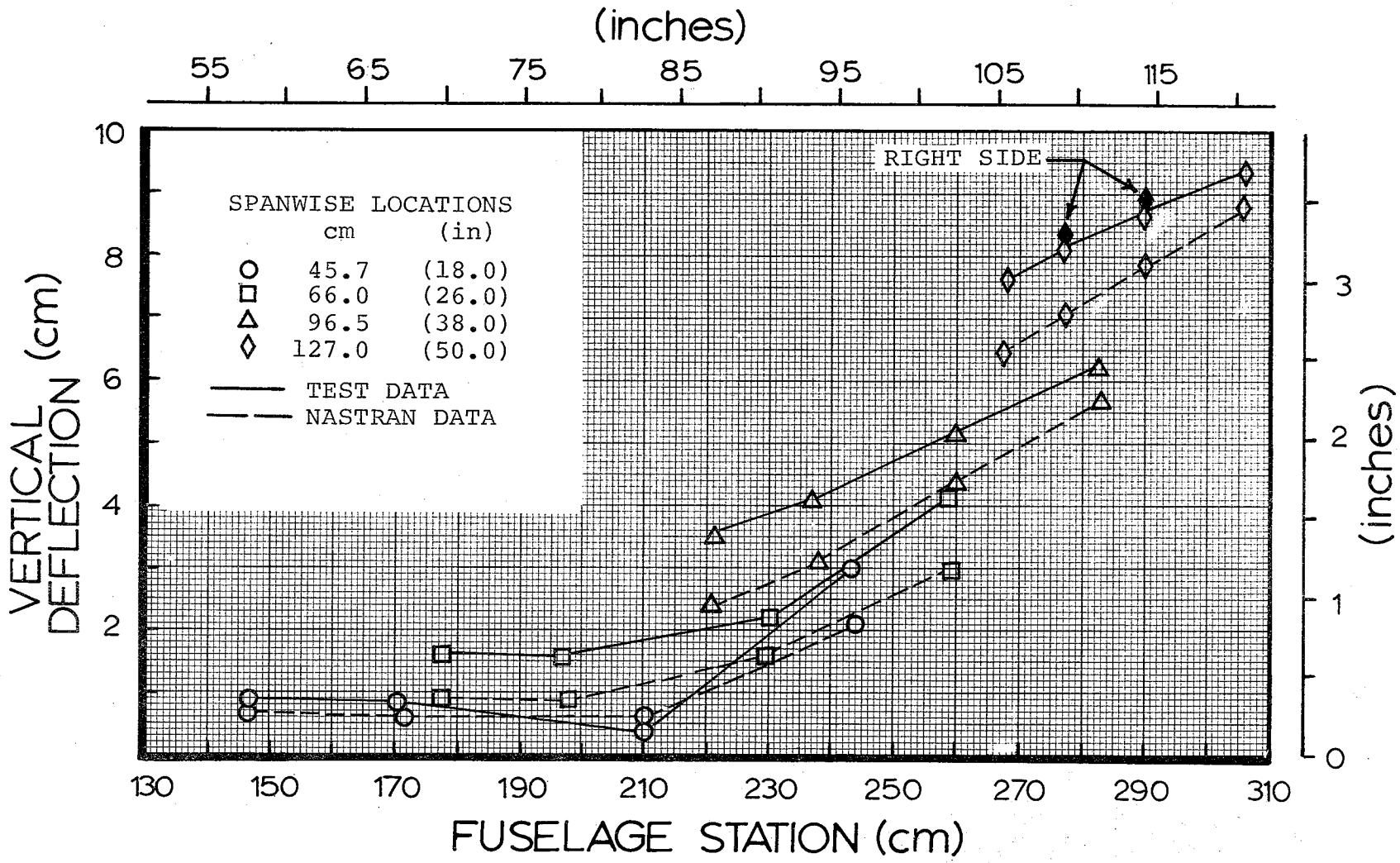

(b) Canard, left side (except as noted).

Figure 9. Concluded.

1. Report No.	2. Government Accession No.	3. Recipient's Catalog No.
NASA TM-81354		

4. Title and Subtitle	5. Report Date
DESCRIPTION OF THE HiMAT TAILORED COMPOSITE STRUCTURE AND LABORATORY MEASURED VEHICLE SHAPE UNDER LOAD	February 1981
	6. Performing Organization Code 533-03-14
7. Author(s) Richard C. Monaghan	8. Performing Organization Report No. H-1144
	10. Work Unit No.
9. Performing Organization Name and Address NASA Dryden Flight Research Center P.O. Box 273 Edwards, California 93523	11. Contract or Grant No.
	13. Type of Report and Period Covered Technical Memorandum
12. Sponsoring Agency Name and Address National Aeronautics and Space Administration Washington, D.C. 20546	14. Sponsoring Agency Code

15. Supplementary Notes

16. Abstract

One of the major design features of the highly maneuverable aircraft technology (HiMAT) vehicle is an aeroelastically tailored outer wing and canard. A detailed description of these structures along with a general description of the overall structure of the vehicle is provided. Test data in the form of laboratory measured twist under load and predicted twist from the HiMAT NASTRAN structural design program are compared. The results of this comparison indicate that the measured twist is generally less than the NASTRAN predicted twist. These discrepancies in twist predictions are attributed, at least in part, to the inability of current analytical composite materials programs to provide sufficiently accurate properties of matrix dominated laminates for input into structural programs such as NASTRAN.

17. Key Words (Suggested by Author(s))	18. Distribution Statement
HiMAT structure Composite structure Aeroelastic tailoring	Unclassified-Unlimited Subject category 05

19. Security Classif. (of this report)	20. Security Classif. (of this page)	21. No. of Pages	22. Price*
Unclassified	Unclassified	62	$7.00

For sale by the National Technical Information Service, Springfield, Virginia 22161